Table 3 Multinominal logistic regression analysis of the association between prescription frequencies of medical drugs for CKD with primary care physicians' age group, specialty, workplace and the existence of a dialysis center at their workplace

	Association of prescription frequency			
	Age	Speciality	Workplace	Dialysis center
Ca inhibitors	0.27	<0.01**	0.62	0.13
ACEIs	0.23	0.04	<0.01**	0.88
ARBs	0.11	0.06	<0.01**	0.12
Statins	0.07	0.77	0.17	0.02
Anti-platelets	0.53	0.80	0.36	0.10
Epo	0.23	0.58	<0.01**	<0.01**
AST-120	0.20	0.38	0.04	0.20
Vitamin D	0.23	0.58	<0.01**	<0.01**
$NaHCO_3$	0.80	0.10	0.31	<0.01**

was seen throughout. The small sample number of pediatricians in the present study ($n = 12$) may affect these results. Further large-scale studies are necessary to investigate prescription patterns of primary care physician in pediatricians for CKD.

More than 30 % of patients already have anemia (hemoglobin (Hb) levels <12 g/dL) by stage 3 CKD, and many patients develop anemia before being diagnosed with CKD [12]. Anemia increases the risk for cardiovascular disease and all-cause mortality in CKD patients [13]. These lines of evidence suggest that the treatment and management of anemia in CKD patients are important to improve the prognosis of CKD. Although there were differences in the prescription frequency of Epo among the workplace and the existence of a dialysis center at the workplace in the present study, the CKD primary care physicians appeared to manage anemia well in CKD patients considering the high prescription frequency of Epo (>70 %: high + moderate prescription rate). In addition, the fact that the prescription frequency was positively associated with the existence of a dialysis center at their workplace also suggested that the number of advanced-stage CKD patients who required Epo was high and they were treated well at medical establishments with a dialysis center.

Statins (>70 %: high + moderate prescription rate) were reported to be highly prescribed in CKD in this study by primary care physicians irrespective of their age group, specialty, workplace, and the existence of a dialysis center at their workplace. The effectiveness of lipid lowering on the reduction of cardiovascular endpoints or the progression of renal disease is under investigation and requires further evaluation [14, 15]. Evidence about the use of statins in CKD should be established to guide CKD primary care physicians in the near future.

AST-120, an adsorbent of uremic toxins, has been reported to delay the progression of renal failure [16] and is widely used in Japan. In the present study, AST-120 was reported to be moderately (73.5 %, high + moderate prescription rate) prescribed in CKD patients by primary care physicians irrespective of their age group, specialty, workplace and the existence of a dialysis center at their workplace. These results suggest that AST-120 is widely used and prescribed in advanced-stage CKD patients.

The overall reported prescription frequencies of vitamin D (45.5 %, high + moderate prescription rate) and $NaHCO_3$ (20.6 %, high + moderate prescription rate) by CKD primary care physicians were low in the present study. Vitamin D was less likely to be prescribed by CKD primary care physicians whose workplace was a university hospital or a clinic than by those working in a polyclinic hospital or hospital. It was prescribed more by CKD primary care physicians with a dialysis center at their workplace. $NaHCO_3$ was also prescribed more by CKD primary care physicians with a dialysis center at their workplace. These results may suggest that vitamin D and $NaHCO_3$ were prescribed more in advanced-stage CKD patients including maintenance dialysis patients. Another possibility for the overall low prescription frequencies of vitamin D and $NaHCO_3$ may be due to the fact that primary care physicians in the present study referred to a nephrologist about management of CKD patients before using these drugs; this trend may increase in primary care physicians who work at a university hospital or clinic compared with those working at a polyclinic hospital or hospital. Recent studies showed that metabolic acidosis presents early in CKD and could be associated with decreasing renal function [17]. Vitamin D therapy can slow the progression of secondary hyperparathyroidism, which begins at an early stage of CKD [18, 19]. These lines of evidence suggested that periodic estimation of the necessity of pharmacological treatment by vitamin D and $NaHCO_3$ is required in CKD patients, even when they are at an early stage. Although we did not evaluate that estimation of metabolic acidosis, electric abnormality, and hyperparathyroidism by CKD primary care physicians in CKD in the present study, the levels of such estimation and treatment may be insufficient considering the reported low prescription frequencies of vitamin D and $NaHCO_3$. Further studies are necessary to investigate the details of the low prescription frequency of vitamin D and $NaHCO_3$ by primary care physicians.

There are several limitations to this study. First, since the study instrument was a mailed self-administered questionnaire, there may be self-selection bias, and it may also contribute to the low response rate (28.2 %) to questionnaire. Second, the primary care physicians in this study may not be a representative population of all primary care

physicians because all medical doctors in this study graduated from one medical university; however, the majority of graduates of this medical university work as primary care physicians. Third, the questionnaire did not include definition and classification of CKD; therefore, recognition of CKD by primary physicians in the present study may vary, and may influence their answers. Fourth, the sample number of CKD primary care physicians in pediatrics and surgery was small. This small sample number may affect the analysis results in the present study. Fifth, it should be noted that the results of this study were from a self-administered questionnaire and were not objectively evaluated in terms of prescription frequencies of drugs. Finally, primary care physicians' reports of their own answers may not always be accurate [20]. Further studies will be needed to investigate the prescription pattern of primary care physicians in each CKD stage compared with the actual prescribed dose.

In conclusion, antihypertensives were highly prescribed, and vitamin D and $NaHCO_3$ were less prescribed for CKD by primary care physicians. There were certain associations between the prescribing patterns of primary care physicians for CKD and their specialty, workplace and the existence of a dialysis center at their workplace. Further dissemination and implementation of clinical practice guidelines for CKD [1, 11, 21] for primary care physicians, as well as the partnership between primary care physicians and nephrologists in terms of clinical practice for CKD, are important for improving the management of CKD.

Acknowledgments The authors thank Minami Watanabe, Yuko Suda, Yukari Hoshino, and Aiko Oashi for their excellent assistance.

Conflict of interest The authors declare no conflicts of interest.

References

1. K/DOQI clinical practice guidelines for chronic kidney disease. Evaluation, classification, and stratification. Am J Kidney Dis. 2002;39:S1–266.
2. Levey AS, Eckardt KU, Tsukamoto Y, Levin A, Coresh J, Rossert J, De Zeeuw D, Hostetter TH, Lameire N, Eknoyan G. Definition and classification of chronic kidney disease: a position statement from kidney disease: improving global outcomes (KDIGO). Kidney Int. 2005;67:2089–100.
3. Kappel J, Calissi P. Nephrology: 3. Safe drug prescribing for patients with renal insufficiency. CMAJ. 2002;166:473–7.
4. Gabardi S, Abramson S. Drug dosing in chronic kidney disease. Med Clin N Am. 2005;89:649–87.
5. Lopez-Novoa JM, Martinez-Salgado C, Rodriguez-Pena AB, Lopez-Hernandez FJ. Common pathophysiological mechanisms of chronic kidney disease: therapeutic perspectives. Pharmacol Ther. 2010;128:61–81.
6. Ritz E. Minor renal dysfunction: an emerging independent cardiovascular risk factor. Heart. 2003;89:963–4.
7. Al-Ramahi R. Medication prescribing patterns among chronic kidney disease patients in a hospital in Malaysia. Saudi J Kidney Dis Transpl. 2012;23:403–8.
8. Roy P, Bouchard J, Amyot R, Madore F. Prescription patterns of pharmacological agents for left ventricular systolic dysfunction among hemodialysis patients. Am J Kidney Dis. 2006;48:645–51.
9. Vupputuri S, Batuman V, Muntner P, Bazzano LA, Lefante JJ, Whelton PK, He J. Effect of blood pressure on early decline in kidney function among hypertensive men. Hypertension. 2003;42:1144–9.
10. Perkovic V, Ninomiya T, Arima H, Gallagher M, Jardine M, Cass A, Neal B, Macmahon S, Chalmers J. Chronic kidney disease, cardiovascular events, and the effects of perindopril-based blood pressure lowering: data from the progress study. J Am Soc Nephrol. 2007;18:2766–72.
11. K/DOQI clinical practice guidelines on hypertension and antihypertensive. Agents in chronic kidney disease. Am J Kidney Dis. 2004;43:S1–290.
12. McClellan W, Aronoff SL, Bolton WK, Hood S, Lorber DL, Tang KL, Tse TF, Wasserman B, Leiserowitz M. The prevalence of anemia in patients with chronic kidney disease. Curr Med Res Opin. 2004;20:1501–10.
13. Vlagopoulos PT, Tighiouart H, Weiner DE, Griffith J, Pettitt D, Salem DN, Levey AS, Sarnak MJ. Anemia as a risk factor for cardiovascular disease and all-cause mortality in diabetes: the impact of chronic kidney disease. J Am Soc Nephrol. 2005;16:3403–10.
14. Wanner C, Krane V, Marz W, Olschewski M, Mann JF, Ruf G, Ritz E. Atorvastatin in patients with type 2 diabetes mellitus undergoing hemodialysis. N Engl J Med. 2005;353:238–48.
15. Shoji T, Masakane I, Watanabe Y, Iseki K, Tsubakihara Y. Elevated non-high-density lipoprotein cholesterol (non-HDL-C) predicts atherosclerotic cardiovascular events in hemodialysis patients. Clin J Am Soc Nephrol. 2011;6:1112–20.
16. Hatakeyama S, Yamamoto H, Okamoto A, Imanishi K, Tokui N, Okamoto T, Suzuki Y, Sugiyama N, Imai A, Kudo S, Yoneyama T, Hashimoto Y, Koie T, Kaminura N, Saitoh H, Funyu T, Ohyama C. Effect of an oral adsorbent, AST-120, on dialysis initiation and survival in patients with chronic kidney disease. Int J Nephrol. 2012;2012:376128.
17. Ortega LM, Arora S. Metabolic acidosis and progression of chronic kidney disease: incidence, pathogenesis, and therapeutic options. Nefrologia. 2012;32:724–30.
18. Levin A, Bakris GL, Molitch M, Smulders M, Tian J, Williams LA, Andress DL. Prevalence of abnormal serum vitamin D, PTH, calcium, and phosphorus in patients with chronic kidney disease: results of the study to evaluate early kidney disease. Kidney Int. 2007;71:31–8.
19. Zehnder D, Landray MJ, Wheeler DC, Fraser W, Blackwell L, Nuttall S, Hughes SV, Townend J, Ferro C, Baigent C, Hewison M. Cross-sectional analysis of abnormalities of mineral homeostasis, vitamin D and parathyroid hormone in a cohort of predialysis patients. The chronic renal impairment in Birmingham (CRIB) study. Nephron Clin Pract. 2007;107:c109–16.
20. McPhee SJ, Richard RJ, Solkowitz SN. Performance of cancer screening in a university general internal medicine practice: comparison with the 1980 American cancer society guidelines. J Gen Intern Med. 1986;1:275–81.
21. Evidence-based practice guideline for the treatment of CKD. Clin Exp Nephrol. 2009; 13:537–566.

Clin Exp Nephrol
DOI 10.1007/s10157-013-0879-4

ORIGINAL ARTICLE

Clinical impact of albuminuria and glomerular filtration rate on renal and cardiovascular events, and all-cause mortality in Japanese patients with type 2 diabetes

Takashi Wada · Masakazu Haneda · Kengo Furuichi · Tetsuya Babazono · Hiroki Yokoyama · Kunitoshi Iseki · Shin-ichi Araki · Toshiharu Ninomiya · Shigeko Hara · Yoshiki Suzuki · Masayuki Iwano · Eiji Kusano · Tatsumi Moriya · Hiroaki Satoh · Hiroyuki Nakamura · Miho Shimizu · Tadashi Toyama · Akinori Hara · Hirofumi Makino · The Research Group of Diabetic Nephropathy, Ministry of Health, Labour, and Welfare of Japan

Received: 3 August 2013 / Accepted: 21 September 2013

Abstract
Background The number of patients suffering from diabetic nephropathy resulting in end-stage kidney disease is increasing worldwide. In clinical settings, there are limited data regarding the impact of the urinary albumin-to-creatinine ratio (UACR) and reduced estimated glomerular filtration rate (eGFR) on renal and cardiovascular outcomes and all-cause mortality.
Methods We performed a historical cohort study of 4328 Japanese participants with type 2 diabetes from 10 centers. Risks for renal events (requirement for dialysis or transplantation, or half reduction in eGFR), cardiovascular events (cardiovascular death, nonfatal myocardial infarction, or nonfatal stroke), and all-cause mortality were assessed according to UACR and eGFR levels.
Results During follow-up (median 7.0 years, interquartile range 3.0–8.0 years), 419 renal events, 605 cardiovascular events and 236 deaths occurred. The UACR levels increased the risk and the adjusted hazard ratios for these three events. In addition to the effects of UACR levels, eGFR stages significantly increased the adjusted hazard ratios for renal events and all-cause mortality, especially in

T. Wada · K. Furuichi · M. Shimizu · T. Toyama · A. Hara
Division of Nephrology, Kanazawa University Hospital, Kanazawa, Japan

T. Wada (✉)
Division of Nephrology, Department of Laboratory Medicine, Institute of Medical, Pharmaceutical and Health Sciences, Faculty of Medicine, Kanazawa University, Kanazawa, 13-1 Takara-machi, Kanazawa 920-8641, Japan
e-mail: twada@m-kanazawa.jp

M. Haneda
Department of Medicine, Asahikawa Medical University, Asahikawa, Japan

K. Furuichi · M. Shimizu · T. Toyama · A. Hara
Department of Disease Control and Homeostasis, Institute of Medical, Pharmaceutical and Health Sciences, Kanazawa University, Kanazawa, Japan

T. Babazono
Division of Nephrology and Hypertension, Diabetes Center, Tokyo Women's Medical University School of Medicine, Tokyo, Japan

H. Yokoyama
Jiyugaoka Medical Clinic, Internal Medicine, Obihiro, Japan

K. Iseki
Dialysis Unit, University Hospital of the Ryukyus, Nishihara, Okinawa, Japan

S. Araki
Department of Medicine, Shiga University of Medical Science, Otsu, Shiga, Japan

T. Ninomiya
Department of Medicine and Clinical Science, Graduate School of Medical Sciences, Kyushu University, Fukuoka, Japan

S. Hara
Center of Health Management, Toranomon Hospital, Tokyo, Japan

Y. Suzuki
Health Administration Center, Niigata University, Niigata, Japan

M. Iwano
Division of Nephrology, Department of General Medicine, University of Fukui, Fukui, Japan

E. Kusano
Division of Nephrology, Department of Internal Medicine, Jichi Medical University, Tochigi, Japan

Published online: 17 October 2013

patients with macroalbuminuria. Diabetic nephropathy score, based on the prognostic factors, well predicted incidence rates per 1000 patient/year for each event.
Conclusions Increased UACR levels were closely related to the increase in risks for renal, cardiovascular events and all-cause mortality in Japanese patients with type 2 diabetes, whereas the association between high levels of UACR and reduced eGFR was a strong predictor for renal events.

Keywords Diabetic nephropathy · Chronic kidney disease · Albuminuria · Cardiovascular disease · Mortality · Glomerular filtration rate

Introduction

Diabetic nephropathy is a leading cause of end-stage kidney (renal) disease (ESKD or ESRD) worldwide [1]. In addition, cardiovascular diseases and deaths increase in patients with diabetic nephropathy before and after dialysis [2–4]. Therefore, to determine and manage risk factors for progression of renal and cardiovascular outcomes and mortality is of importance to prolong the life expectancy of diabetic patients.

A high urinary albumin-to-creatinine ratio (UACR) and low estimated glomerular filtration rate (eGFR) have been believed to be predictors for diabetic ESKD and death [5–7]. Kidney Disease Improving Global Outcomes (KDIGO) provided a new classification for chronic kidney disease (CKD) by adding stages that stratified urinary albumin excretion as well as eGFR and emphasizing clinical diagnosis [8]. This new classification, mainly based on the collaborative meta-analysis of general population cohorts [8], has shed light on prognosis assigned by clinical diagnosis, stage, and other key factors relevant to renal and cardiovascular outcomes. However, the clinical impact of UACR levels in combination with eGFR on outcomes in Japanese patients with diabetic nephropathy needs to be confirmed. Therefore, deeper clinical insights of UACR along with GFR are required to provide a key for the pathogenesis and outcomes of progressive renal complications, and associated cardiovascular events in type 2 diabetic patients.

Here we examined the prognostic value of UACR and eGFR for renal events, cardiovascular events and all-cause mortality in Japanese patients with type 2 diabetes. Furthermore, we proposed a diabetic nephropathy score for predicting prognosis in diabetic patients.

Subjects and methods

Subjects

This study was a historical cohort consisting of 4814 Japanese patients with type 2 diabetes who were treated by trained physicians at 10 centers between 1985 and 2010. Four hundred and fifty-nine patients were excluded because of age <18 ($n = 6$), follow-up <1 year ($n = 151$) and no measurement of urinary albumin or HbA1c or blood pressure (BP) ($n = 329$), leaving 4328 Japanese patients to be enrolled in this study. Patients with secondary diabetes, renal transplantation or dialysis were also excluded.

This study was conducted according to the ethical guidelines for epidemiological research designed by the Japanese Ministry of Education, Culture, Sports, Science and Technology and Ministry of Health, Labour, and Welfare (http://www.lifescience.mext.go.jp/files/pdf/n796_01.pdf).

The study design was included in a comprehensive protocol of retrospective study at the Division of Nephrology, Kanazawa University Hospital approved by Kanazawa University ethical committee (approval number 815).

Follow-up and assessments

Type 2 diabetes was defined according to the Japan Diabetes Society (JDS) criteria [9]. In this historical cohort study, UACR and eGFR were also determined. Measurement of UACR, by a turbidimetric immunoassay at each laboratory, was performed on spot urine samples at baseline. Serum creatinine was measured at baseline, at subsequent yearly intervals, and at the end of follow-up. Serum and urinary concentrations of creatinine were measured by an enzymatic method, and eGFR was estimated using the equation proposed by the Japanese Society of Nephrology [10]. Both UACR and serum creatinine were measured at local laboratories. At each study visit, blood pressure (BP) was measured in the sitting position. Hypertension was defined as BP $\geq$ 140/90 mmHg or

T. Moriya
Health Care Center, Kitasato University, Sagamihara, Japan

H. Satoh
Department of Nephrology, Hypertension, Diabetology, and Metabolism, Fukushima Medical University, Fukushima, Japan

H. Nakamura
Department of Environmental and Preventive Medicine, Institute of Medical, Pharmaceutical and Health Sciences, Kanazawa University, Kanazawa, Japan

H. Makino
Department of Medicine and Clinical Science, Okayama University Graduate School of Medicine, Dentistry and Pharmaceutical Sciences, Okayama, Japan

current use of antihypertensive drugs. Non-fasting blood samples were obtained for measurements of HbA1c and lipid levels at local laboratories. HbA1c was measured and standardized by the JDS (normal range 4.3–5.8 %) and certified by the US National Glycohemoglobin Standardization Program (National Glycohemoglobin Standardization Program, NGSP; NGSP = JDS + 0.4) [9].

UACR and GFR categories

Based on the new classification of CKD [8], the albuminuria category was classified at baseline as normoalbuminuria (<30 mg/g), microalbuminuria (≥30 and <300 mg/g), and macroalbuminuria (≥300 mg/g). In addition, baseline eGFR levels were divided into six categories: ≥90, 60–89, 45–59, 30–44, 15–29 and <15 ml/min per 1.73 m^2. Patients examined in this study were categorized and assessed based on the above classifications.

Outcomes

The main outcomes of this study were renal events (requirement for dialysis or transplantation, or half reduction in eGFR), cardiovascular events (cardiovascular death, nonfatal myocardial infarction, or nonfatal stroke), and all-cause mortality death. These conditions corresponded to the International Classification of Diseases, 11th version (http://www.who.int/classification/icd/en/). Definitions for nonfatal myocardial infarction and nonfatal stroke are given elsewhere [11]. Patients were referred to cardiologists, neurosurgeons, neurologists or else to confirm diagnoses. Only the first event of the relevant outcome type was included in each analysis and the last day of the observation period was also noted if there were no incidences.

Statistical analysis

Data are expressed as mean ± SD or median (interquartile range). Incidence rates of renal events, cardiovascular events, and all-cause death for different categories were calculated. Cox proportional hazards analysis was used to compute hazard ratios and 95 % confidence intervals (CI) to assess the impact of albuminuria and eGFR on the outcomes by using the group with eGFR ≥60 ml/min per 1.73 m^2 and/or the group with normoalbuminuria (<30 mg/g) as the reference [8]. In multivariate analysis, adjustment for risk factors for renal events, cardiovascular events, or all-cause mortality included age, gender, HbA1c, and systolic BP. A p value <5 % was considered significant. p values for trend tests examined whether UACR and eGFR levels were associated with increased hazard ratios. Trend tests across increasing risks for renal, cardiovascular events and all-cause mortality are stratified by factors for diabetic nephropathy score.

All analyses were performed with the statistical software package SPSS (SPSS Japan, Tokyo, Japan).

Results

Baseline characteristics

Table 1 shows the baseline characteristics of patients examined in this study. The 4328 patients were distributed according to CKD stage and were followed until the onset of the first event or the end of the observation period (Table 1).

Incidence of numbers of patients of each event

During a median follow-up of 7.0 years (interquartile range 3.0–8.0 years), 419 renal events, 605 cardiovascular events and 236 deaths occurred, which were stratified by stages of renal function and levels of UACR with each event (Table 2). The incidence rates of each outcome per 1000 person-years were 19.8 for renal events, 23.3 for cardiovascular events and 8.4 for all-cause mortality. The incidence of each event increased with worsening of UACR levels and eGFR stages. Of importance, high incidence rates were noted in patients with macroalbuminuria plus reduced eGFR, especially for renal events (Table 2).

Risk for renal events, cardiovascular events, and all-cause mortality stratified by albuminuria and eGFR

Risks for renal events, cardiovascular events and all-cause mortality were evaluated by Cox proportional hazards analysis. The estimates were adjusted for age, gender, HbA1c, and systolic BP. The adjusted hazard ratios for renal events were 3.21 (95 % CI 2.31–4.47) for microalbuminuric patients and 21.86 (95 % CI 16.15–29.59) for macroalbuminuric patients as compared to normoalbuminuric patients as reference. Similarly, the adjusted hazard ratios for cardiovascular events and all-cause mortality were 1.38 (95 % CI 1.14–1.67) and 1.37 (95 % CI 0.99–1.89) for microalbuminuric patients and 2.05 (95 % CI 1.61–2.58) and 3.60 (95 % CI 2.53–5.20) for macroalbuminuric patients as compared to reference, respectively. Interestingly, UACR levels had the most significant impact on renal events. In addition to the effects of UACR levels, eGFR stages significantly increased the adjusted hazard ratios for renal events in patients with macroalbuminuria (Table 3). In Table 3, hazard ratios for cardiovascular events increased in patients with a higher UACR. In

Table 1 Baseline characteristics of participants ($n = 4328$)

Variable	All	Normoalbuminuria	Microalbuminuria	Macroalbuminuria	p For trend
N	4328	2679	1115	534	
Age (years; mean [SD])	60.2 (11.6)	59.5 (11.4)	61.9 (11.5)	59.8 (12.0)	<0.001
Male (*n* [%])	2546 (58.8)	1531 (57.1)	656 (58.8)	359 (67.2)	<0.001
Kidney factors					
UACR (mg/g; median [IQR])	18.2 (8.6–66.6)	10.2 (6.5–16.4)	66.6 (42.6–121.3)	994.8 (518.5–2272.5)	<0.001
eGFR (ml/min/1.73 m^2; mean [SD])	77.0 (25.9)	81.3 (23.8)	76.4 (25.3)	56.9 (28.0)	<0.001
eGFR ≥90 (*n* [%])	1201 (27.7)	839	297	65	
eGFR 60–89 (*n* [%])	2051 (47.4)	1371	530	150	
eGFR 45–59 (*n* [%])	642 (14.8)	345	174	123	
eGFR 30–44 (*n* [%])	311 (7.2)	109	100	102	
eGFR 15–29 (*n* [%])	117 (2.7)	15	14	88	
eGFR <15 (*n* [%])	6 (0.1)	0	0	6	
BP (mmHg)					
Systolic BP (mean [SD])	131.0 (18.6)	127.2 (16.6)	134.2 (18.4)	143.0 (22.0)	<0.001
Diastolic BP (mean [SD])	74.3 (18.0)	73.3 (20.7)	74.8 (11.8)	78.1 (13.1)	<0.001
Other major risk factors					
HbA1c (%; mean [SD])	7.6 (1.7)	7.5 (1.7)	7.8 (1.7)	7.9 (1.8)	<0.001
Total cholesterol (mg/dL; mean [SD])	205.2 (35.9)	205.3 (34.1)	202.2 (33.9)	214.2 (50.2)	0.925
Body mass index (kg/m^2; mean [SD])	25.3 (4.2)	25.1 (4.2)	25.5 (4.2)	25.4 (4.8)	0.098

Table 2 Number of patients and incidence rates of each outcome stratified by stages of eGFR and albuminuria

UACR	eGFR (ml/min/1.73 m^2)					
	>90	60–89	45–59	30–44	15–29	<15
Renal events (RRT or halving reduced eGFR)						
Normoalbuminuria	58 (4.2)		4 (2.3)	3 (6.9)	1 (21.3)	0
Microalbuminuria	31 (17.2)	41 (13.1)	15 (18.0)	10 (21.0)	1 (25.6)	0
Macroalbuminuria	20 (59.5)	62 (87.7)	56 (126.7)	54 (193.5)	61 (309.6)	2 (250.0)
Cardiovascular events						
Normoalbuminuria	229 (16.2)		40 (23.1)	14 (33.0)	1 (18.9)	0
Microalbuminuria	31 (16.1)	95 (28.7)	33 (32.6)	28 (56.1)	2 (43.5)	0
Macroalbuminuria	7 (17.2)	41 (44.6)	30 (44.3)	30 (64.2)	23 (57.9)	1 (100.0)
All-cause mortality						
Normoalbuminuria	70 (4.7)		26 (13.8)	4 (8.2)	4 (67.8)	0
Microalbuminuria	11 (5.4)	32 (8.9)	13 (11.9)	5 (8.5)	6 (117.6)	0
Macroalbuminuria	6 (14.4)	13 (12.3)	19 (24.6)	13 (23.6)	12 (26.8)	2 (142.9)

Number of patients (incidence rates per 1000 person-years)

RRT renal replacement therapy

addition, our results showed that there was a slight increase in the hazard ratios of cardiovascular events based on UACR levels plus co-existing reduced eGFR, especially in patients with microalbuminuria based on p for trend. In contrast, all-cause mortality was strongly associated with reduced eGFR <30 ml/min per 1.73 m^2, and the presence of macroalbuminuria even with preserved eGFR. The present study also revealed that normoalbuminuric renal insufficient diabetic patients did not have relatively poor outcomes for renal events. Table 4 highlights the impact of low GFR and/or UACR on three distinct outcomes.

The clinical significance of diabetic nephropathy score in predicting the prognoses of renal events, cardiovascular events, and all-cause mortality

Considering the results of univariable and multivariable analyses, weighted arbitrary scores were allocated to each

Table 3 Hazard ratios based on CKD stages for each outcome

UACR	eGFR (ml/min/1.73 m^2)						*p* for trend (eGFR)
	>90	60–89	45–59	30–44	15–29	<15	
Renal events (RRT or halving reduced eGFR)							
Normoalbuminuria	1.00 (Reference)	1.00 (Reference)	0.69 (0.24–1.98)	1.83 (0.53–6.31)	11.59 (1.43–93.78)	NA	0.85
Microalbuminuria	3.31 (2.07–5.28)	3.04 (1.98–4.68)	3.36 (1.63–6.93)	3.10 (1.41–6.83)	3.60 (0.42–31.28)	NA	0.60
Macroalbuminuria	11.14 (5.87–21.17)	15.64 (10.30–23.74)	33.37 (20.58–50.91)	41.36 (25.09–68.16)	71.58 (40.41–126.80)	NA	<0.01
p for trend (albuminuria)	<0.01	<0.01	<0.01	<0.01	0.06	NA	
Cardiovascular events							
Normoalbuminuria	1.00 (Reference)	1.00 (Reference)	1.05 (0.73–1.49)	1.30 (0.74–2.28)	0.42 (0.06–3.06)	NA	0.46
Microalbuminuria	1.01 (0.69–1.49)	1.48 (1.15–1.90)	1.33 (0.89–2.00)	1.85 (1.20–2.85)	0.47 (0.11–1.97)	NA	0.04
Macroalbuminuria	1.28 (0.56–2.94)	2.10 (1.46–3.02)	1.85 (1.23–2.78)	2.37 (1.55–3.63)	2.09 (1.26–3.45)	12.76 (0.95–171.19)	0.20
p for trend (albuminuria)	0.81	<0.01	0.09	0.45	0.17	NA	
All-cause mortality							
Normoalbuminuria	1.00 (Reference)	1.00 (Reference)	1.67 (1.02–2.74)	1.22 (0.43–3.46)	8.19 (2.65–25.34)	NA	<0.01
Microalbuminuria	1.51 (0.78–2.95)	1.44 (0.92–2.24)	1.22 (0.63–2.35)	0.84 (0.31–2.26)	8.36 (2.81–24.90)	NA	0.04
Macroalbuminuria	4.37 (1.70–11.24)	1.92 (0.97–3.79)	4.84 (2.72–8.62)	4.09 (2.00–8.34)	6.16 (2.80–13.56)	70.57 (3.65–1363.68)	0.06
p for trend (albuminuria)	0.01	0.01	0.01	0.02	0.80	NA	

The estimates are adjusted for age, gender, HbA1c, systolic BP

RRT renal replacement therapy, *NA* not available

Table 4 Hazard ratios based on levels of UACR and eGFR for each outcome

UACR	eGFR (ml/min/1.73 m^2)		
	>60	30–59	<30
Renal events (RRT or halving reduced eGFR)			
Normoalbuminuria	1.00 (Reference)		49.82 (29.9–83.0)
Microalbuminuria	3.26 (2.34–4.55)		
Macroalbuminuria	13.6 (9.3–20.0)	33.0 (22.7–48.2)	
Cardiovascular events			
Normoalbuminuria	1.00 (Reference)		1.54 (1.00–2.39)
Microalbuminuria	1.40 (1.16–1.69)		
Macroalbuminuria	1.90 (1.36–2.65)	2.09 (1.54–2.84)	
All-cause mortality			
Normoalbuminuria	1.00 (Reference)		7.08 (4.16–12.05)
Microalbuminuria	1.30 (0.93–1.81)		
Macroalbuminuria	2.34 (1.35–4.04)	4.59 (2.90–7.25)	

The estimates are adjusted for age, gender, HbA1c, systolic BP

selected variable on the basis of each odds ratio (OR), and we defined a summation of scores as a new risk scoring system as the diabetic nephropathy score. We evaluated the diabetic nephropathy score for predicting the prognoses of renal events, cardiovascular events, and all-cause mortality. Each prognostic factor has a score and the maximum score is 6—microalbuminuria = 1, macroalbuminuria = 2, eGFR <45 ml/min per 1.73 m^2 = 1, age ≥60 years = 1, systolic BP >130 mmHg = 1, and HbA1c (NGSP) ≥6.9 % = 1. This score put stress on amounts of UACR. Importantly, this simple score well predicted the incidence rates per 1000 patient/year for each event (Table 5).

Discussion

In this study we examined the clinical impact of UACR as well as the evaluation of GFR on outcomes in diabetic patients. We now report that increased urinary albumin excretion was strongly associated with risks for renal

Table 5 Diabetic nephropathy score reflects diabetic outcomes

	Renal events (RRT or halving reduced eGFR)				Cardiovascular events				All-cause mortality			
Score	Number of patients	Number of incidents	Rate per 1000 patient-years	95 % CI	Number of patients	Number of incidents	Rate per 1000 patient-years	95 % CI	Number of patients	Number of incidents	Rate per 1000 patient-years	95 % CI
0	204	0	0.0		204	2	1.4	0.2–5.1	204	0	0.0	
1	902	18	3.1	1.9–5.0	954	58	9.7	7.4–12.6	954	13	2.1	1.1–3.6
2	1228	54	6.9	5.2–9.0	1,310	174	21.4	18.4–24.9	1310	71	8.1	6.3–10.3
3	952	96	16.6	13.4–20.0	1,017	161	26.2	22.3–30.6	1017	62	9.4	7.2–12.0
4	471	118	46.6	38.5–56.0	532	116	39.0	32.2–46.8	532	45	13.4	9.8–18.0
5	213	93	103.8	83.8–127.0	238	71	60.5	47.3–76.3	238	35	25.5	17.7–35.4
6	61	40	216.2	154.5–294.0	73	23	80.4	51.0–120.7	73	10	28.1	13.5–51.7
p for trend			<0.001				<0.001				<0.001	

events, cardiovascular events and deaths in Japanese patients with type 2 diabetes. Of note, eGFR stages significantly increased the adjusted hazard ratios for renal events, especially when co-existing with macroalbuminuria, while patients with normoalbuminuria had relatively low risks for renal events. All-cause mortality was strongly associated with reduced eGFR <30 ml/min per 1.73 m^2 and the presence of macroalbuminuria even with preserved eGFR. However, the association between normoalbuminuria and reduced eGFR showed relatively low risks for cardiovascular events in the cohort of the Japanese population with type 2 diabetes. These findings suggested that diabetic patients with macroalbuminuira and low GFR had risks for adverse outcomes, even though UACR levels and eGFR had distinct clinical impacts on each event, respectively. Finally, the diabetic nephropathy score based on our present study may be useful for predicting the prognoses of outcomes in diabetic patients.

The present study has clearly shown that renal insufficiency plus the presence of macroalbuminuria accelerated risks for adverse outcomes, especially renal events. Recently, KDIGO reported the definition, classification and prognosis of CKD based both on estimated GFR and urinary levels of albumin excretion, emphasizing that a decrease in GFR as well as macroalbuminuria is important for renal outcomes of CKD [8]. In addition, the Action in Diabetes and Vascular disease: preterAx and diamicroN-MR Controlled Evaluation (ADVANCE) study reported that reduced eGFR with macroalbuminuria was associated with a higher risk for renal events [6]. Interestingly, the Casale Monferrato study revealed that macroalbuminuira was the main predictor of mortality, independently of both eGFR and cardiovascular risk factors [12]. In contrast, reduced eGFR did not increase the adjusted hazard ratio for renal events even in patients with microalbuminuria. This may be partly because the number of microalbuminuric patients with reduced GFR having renal events was relatively small as shown in Table 2. Collectively, these findings suggest that the assessment of macroalbuminuria as well as levels of eGFR may enable us to predict high risk for renal events.

The association between UACR and reduced eGFR showed relatively low risks for cardiovascular events, even though the incidence rate of cardiovascular events was 23.3, which was almost comparable to that observed in the Japan Diabetes Complications Study (JDCS) [13]. Our results also demonstrated that UACR was closely associated with cardiovascular events in patients with eGFR 60–89 ml/min per 1.73 m^2 and that reduced eGFR was important in microalbuminuric patients based on *p* values for trend. Of note, Yokoyama et al. recently reported that the risk for cardiovascular events was associated with progression of UACR stage in type 2 Japanese diabetic

patients [14]. In contrast, reduced eGFR was a high risk for developing cardiovascular endpoints (cardiovascular death, new admissions due to to angina, myocardial infarction, stroke, revascularization or heart failure) and all-cause mortality independent of UACR [15]. Interestingly, the Second Nord-Trøndelag Health (HUNT II) study [16] reported that reduced eGFR with higher UACR was associated with a higher risk for cardiovascular events. This discrepancy compared to our present study may be partly because the number of patients with cardiovascular events in the present study was relatively small as shown in Table 2. Further studies will be required to examine this discrepancy.

This study also revealed that normoalbuminuric renal insufficient diabetic patients did not have relatively poor renal outcomes. In fact, the percentage of diabetic patients with normoalbuminuria and low eGFR is supposed to be relatively common in clinical settings. In this aspect, Yokoyama et al. [17] described that the proportion of subjects with low eGFR (<60 ml/min per 1.73 m^2) and normoalbuminuria was 11.4 % of type 2 diabetic patients examined (262/2,298). Supporting our notion, Rigalleau et al. [18] reported that risk for renal progression in such patients with type 1 or type 2 diabetes is lower. On the contrary, all-cause mortality, not cardiovascular events, was strongly associated with reduced eGFR <30 ml/min per 1.73 m^2 in normoalbuminuric diabetic patients in this present study. Supporting this notion, hazard ratios for all-cause mortality as well as cardiovascular mortality increased in normoalbuminuric diabetic patients with low GFR [19]. The FIELD study also revealed that normoalbuminuric patients with eGFR 30–59 ml/min per 1.73 m^2 had a higher risk of cardiovascular events, cardiovascular death, non-coronary heart disease deaths, death from any cause than normoalbuminuric patients with eGFR ≥60 ml/min per 1.73 m^2 [7]. Interestingly, in the ADVANCE study, patients with normoalbuminuria and eGFR <60 ml/min/1.73 m^2 had a 3.95-fold higher risk for renal events, a 1.33-fold higher risk for cardiovascular events and a 1.85-fold higher risk for cardiovascular death [6]. In contrast, Vlek et al. [20] reported that eGFR <60 ml/min per 1.73 m^2 without UACR mainly influenced the risk of vascular events (hazard ratio 1.50; 1.05–2.15), but did not affect all-cause mortality. Furthermore, in type 2 diabetic patients, eGFR provided no further information for all-cause mortality and cardiovascular mortality in normoalbuminuric patients [14]. Therefore, further studies are needed to determine renal outcomes as well as all-cause mortality in normoalbuminuric diabetic patients with low eGFR.

We proposed a novel diabetic nephropathy score to predict incidence rates per 1000 patient/year for each event. To date, few studies have addressed individual prognostic factors/scores to predict outcomes of diabetic complications in clinical settings. Couchoud et al. [21] reported development and validation of a prognostic score for 6-month mortality in elderly patients starting dialysis for ESKD. Nine risk factors were selected and points assigned for the score were body mass index <18.5 kg/m^2 (2 points), diabetes (1 point), congestive heart failure stages III to IV (2 points), peripheral vascular disease stages III to IV (2 points), dysrhythmia (1 point), active malignancy (1 point), severe behavioral disorder (2 points), total dependency for transfers (3 points) and unplanned dialysis (2 points). These scores effectively predict short-term prognosis among elderly patients, in which approximately 20 % of the patients had diabetic nephropathy. In contrast to this previous study, our simple prognostic scoring system may clearly predict cardiovascular events and all-cause mortality as well as renal events for patients of any age. Even though validation of this score system will be required for other cohorts, this system seems simple and useful for predicting clinical aspects.

To date, UACR levels and reduced eGFR have independently been reported to predict cardiovascular and real outcomes in diabetes [6]. Previously, diabetic patients with microalbuminuria/macroalbuminuira had a risk for adverse outcomes, including cardiovascular events, cardiovascular death, and renal events as reported by the ADVANCE study [6]. Importantly, the present study, consisting of 4328 Japanese patients with type 2 diabetes, was critically different from the ADVANCE study in terms of (1) being a historical cohort study consisting of 10 centers, (2) longer observation period (median 7.0 years), (3) including the assessment of all-cause mortality, (4) including assessment of each event based on the new classification CKD stages, and (5) providing a diabetic nephropathy score to predict the prognoses of renal events, cardiovascular events, and all-cause mortality. Therefore, our present study further revealed the clinical significance of UACR and eGFR on adverse outcomes in diabetic patients.

There are several limitations to this study. First, the lack of histologically proven diabetic nephropathy should be discussed, even though diabetic nephropathy is clinically diagnosed by the presence of microalbuminuria. Second, the low incidence of cardiovascular events may result in a relatively weak statistical power. Furthermore, the lack of data regarding whether enrolled patients have predisposing cardiovascular diseases must be considered. However, this multicenter observational study of 4328 diabetic patients over 7 years may strengthen the present results and increase the accuracy of risk estimation and establishment of a prognostic diabetic nephropathy score.

In conclusion, these results conclude that the presence of microalbuminuria/macroalbuminuria is closely related to the increase in risks for adverse outcomes in Japanese diabetic patients, whereas the association between

macroalbuminuria and reduced eGFR was a strong predictor for renal events. Further studies will be required to validate the prognostic factors and related diabetic nephropathy score by using other cohorts together with future perspectives.

Acknowledgments The authors thank Dr. Yukinari Yamaguchi (Nara Medical University), Dr. Mitsuhiro Yoshimura (Noto General Hospital), and Miyuki Murakami (Kanazawa University) for supporting this study. This study was supported by Grant-in-Aids for Diabetic Nephropathy Research and for Diabetic Nephropathy and Nephrosclerosis Research, from the Ministry of Health, Labour and Welfare of Japan and by the Ministry of Education, Science, Sports and Culture, Japan.

Conflict of interest H. Makino is a consultant for AbbVie, Astellas and Teijin, receives speaker honoraria from Astellas, MSD, Takeda, and Tanabe Mitsubishi, and receives grant support from Astellas, Daiichi Sankyo, Dainippon Sumitomo, MSD, Novo Nodisk and Takeda.

References

1. Parving HH, Mauer M, Fioretto P, Rossing P, Ritz E. Diabetic nephropathy. In: Taal MW, Chertow GM, Marsden PA, Skorecki K, Yu ASL, Brenner BM, editors. The kidney. Philadelphia: Elsevier Saunders; 2012. p. 1411–54.
2. Nakayama M, Sato T, Sato H, Yamaguchi Y, Obara K, Kurihara I, et al. Different clinical outcomes for cardiovascular events and mortality in chronic kidney disease according to underlying renal disease: the Gonryo study. Clin Exp Nephrol. 2010;14:333–9.
3. Foley RN, Culleton BF, Parfrey PS, Harnett JD, Kent GM, Murray DC, et al. Cardiac diseases in diabetic end-stage renal disease. Diabetologia. 1997;40:1307–12.
4. Wada T, Shimizu M, Toyama T, Hara A, Kaneko S, Furuichi K. Clinical impact of albuminuria in diabetic nephropathy. Clin Exp Nephrol. 2012;16:96–101.
5. Berhane AM, Weil EJ, Knowler WC, Nelson RG, Hanson RL. Albuminuria and estimated glomerular filtration rate as predictors of diabetic end-stage renal disease and death. Clin J Am Soc Nephrol. 2011;6:2444–51.
6. Ninomiya T, Perkovic V, de Galan BE, Zoungas S, Pillai A, Jardine M, et al. Albuminuria and kidney function independently predict cardiovascular and renal outcomes in diabetes. J Am Soc Nephrol. 2009;20:1813–21.
7. Drury PL, Ting R, Zannino D, Ehnholm C, Flack J, Whiting M, et al. Estimated glomerular filtration rate and albuminuria are independent predictors of cardiovascular events and death in type 2 diabetes mellitus: the Fenofibrate Intervention and Event Lowering in Diabetes (FIELD) study. Diabetologia. 2011;54:32–43.
8. Levey AS, de Jong PE, Coresh J, El Nahas M, Astor BC, Matsushita K, et al. The definition, classification and prognosis of chronic kidney disease: a KDIGO Controversies Conference report. Kidney Int. 2011;80:17–28.
9. Report of the Committee on the classification and Diagnostic Criteria of Diabetes Mellitus: The committee of the Japan Diabetes Society on the Diagnostic Criteria of Diabetes Mellitus. J Diabetes Invest. 2010;1:212–28.
10. Matsuo S, Imai E, Horio M, Yasuda Y, Tomita K, Nitta K, et al. Revised equations for estimated GFR from serum creatinine in Japan. Am J Kidney Dis. 2009;53:982–92.
11. Yokoyama H, Matsushima M, Kawai K, Hirao K, Oishi M, Sugimoto H, et al. Low incidence of cardiovascular events in Japanese patients with type 2 diabetes in primary care settings; a prospective cohort study. Diabetic Med. 2011;28:1221–8.
12. Bruno G, Merletti F, Bargero G, Novelli G, Melis D, Soddu A, et al. Estimated glomerular filtration rate, albuminuria and mortality in type 2 diabetes: the Casale Monferrato study. Diabetologia. 2007;50:941–8.
13. Sone H, Tanaka S, Tanaka S, Iimuro S, Oida K, Yamasaki Y, et al. Serum level of triglycerides is a potent risk factor comparable to LDL cholesterol for coronary heart disease in Japanese patients with type 2 diabetes: subanalysis of the Japan Diabetes Complications Study (JDCS). J Clin Endocrinol Metab. 2011;96:3448–56.
14. Yokoyama H, Araki S, Haneda M, Matsushima M, Kawai K, Hirao K, et al. Chronic kidney disease categories and renal-cardiovascular outcomes in type 2 diabetes without prevalent cardiovascular disease: a prospective cohort study (JDDM 25). Diabetologia. 2012;55:1911–8.
15. So WY, Kong AP, Ma RC, Ozaki R, Szeto CC, Chan NN, et al. Glomerular filtration rate, cardiorenal end points, and all-cause mortality in type 2 diabetic patients. Diabetes Care. 2006;29:2046–52.
16. Hallan S, Astor B, Romundstad S, Assarød K, Kvenild K, Coresh J. Association of kidney function and albuminuria with cardiovascular mortality in older vs. younger individuals: The HUNT II Study. Arch Intern Med. 2007;167:2490–6.
17. Yokoyama H, Kawai K, Kobayashi M, Japan Diabetes Clinical Data Management Study Group. Microalbuminuria is common in Japanese type 2 diabetic patients: a nationwide survey from the Japan Diabetes Clinical Data Management Study Group (JDDM 10). Diabetes Care. 2007;30:989–92.
18. Rigalleau V, Lasseur C, Raffaitin C, Beauvieux MC, Barthe N, Chauveau P, et al. Normoalbuminuric renal-insufficient diabetic patients: a lower-risk group. Diabetes Care. 2007;30:2034–9.
19. Fox CS, Matsushita K, Woodward M, Bilo HJ, Chalmers J, Heerspink HJ, et al. Association of kidney disease measures with mortality and end-stage renal disease in individuals with and without diabetes: a meta-analysis. Lancet. 2013;381:374.
20. Vlek AL, van der Graaf Y, Spiering W, Algra A, Visseren FL, SMART study group. Cardiovascular events and all-cause mortality by albuminuria and decreased glomerular filtration rate in patients with vascular disease. J Intern Med. 2008;264:351–60.
21. Couchoud C, Labeeuw M, Moranne O, Allot V, Esnault V, Frimat L, et al. A clinical score to predict 6-month prognosis in elderly patients starting dialysis for end-stage renal disease. Nephrol Dial Transplant. 2009;24:1553–61.

Am J Physiol Heart Circ Physiol 302: H1871–H1883, 2012.
First published March 2, 2012; doi:10.1152/ajpheart.00663.2011.

Heart angiotensin II-induced cardiomyocyte hypertrophy suppresses coronary angiogenesis and progresses diabetic cardiomyopathy

Takahiro Masuda,[1] Shigeaki Muto,[1] Genro Fujisawa,[2] Yoshitaka Iwazu,[1] Mariko Kimura,[3] Takahisa Kobayashi,[1] Mutsuko Nonaka-Sarukawa,[3] Nobuhiro Sasaki,[1] Yuko Watanabe,[1] Masami Shinohara,[4] Takashi Murakami,[5] Kazuyuki Shimada,[3] Eiji Kobayashi,[5] and Eiji Kusano[1]

Divisions of [1]Nephrology and [3]Cardiovascular Medicine, Department of Internal Medicine, and [5]Division of Organ Replacement Research, Center for Molecular Medicine, Jichi Medical University, Shimotsuke, Tochigi; [2]Fujisawa Medical Clinic, Kashiwa, Chiba; [4]Planning and Development Section, CLEA Japan, Incorporated, Meguro, Tokyo, Japan

Submitted 5 July 2011; accepted in final form 9 February 2012

Masuda T, Muto S, Fujisawa G, Iwazu Y, Kimura M, Kobayashi T, Nonaka-Sarukawa M, Sasaki N, Watanabe Y, Shinohara M, Murakami T, Shimada K, Kobayashi E, Kusano E. Heart angiotensin II-induced cardiomyocyte hypertrophy suppresses coronary angiogenesis and progresses diabetic cardiomyopathy. *Am J Physiol Heart Circ Physiol* 302: H1871–H1883, 2012. First published March 2, 2012; doi:10.1152/ajpheart.00663.2011.—To examine whether and how heart ANG II influences the coordination between cardiomyocyte hypertrophy and coronary angiogenesis and contributes to the pathogenesis of diabetic cardiomyopathy, we used Spontaneously Diabetic Torii (SDT) rats treated without and with olmesartan medoxomil (an ANG II receptor blocker). In SDT rats, left ventricular (LV) ANG II, but not circulating ANG II, increased at 8 and 16 wk after diabetes onset. SDT rats developed LV hypertrophy and diastolic dysfunction at 8 wk, followed by LV systolic dysfunction at 16 wk, without hypertension. The SDT rat LV exhibited cardiomyocyte hypertrophy and increased hypoxia-inducible factor-1α expression at 8 wk and to a greater degree at 16 wk and interstitial fibrosis at 16 wk only. In SDT rats, coronary angiogenesis increased with enhanced capillary proliferation and upregulation of the angiogenic factor VEGF at 8 wk but decreased VEGF with enhanced capillary apoptosis and suppressed capillary proliferation despite the upregulation of VEGF at 16 wk. In SDT rats, the phosphorylation of VEGF receptor-2 increased at 8 wk alone, whereas the expression of the antiangiogenic factor thrombospondin-1 increased at 16 wk alone. All these events, except for hyperglycemia or blood pressure, were reversed by olmesartan medoxomil. These results suggest that LV ANG II in SDT rats at 8 and 16 wk induces cardiomyocyte hypertrophy without affecting hyperglycemia or blood pressure, which promotes and suppresses coronary angiogenesis, respectively, via VEGF and thrombospondin-1 produced from hypertrophied cardiomyocytes under chronic hypoxia. Thrombospondin-1 may play an important role in the progression of diabetic cardiomyopathy in this model.

angiogenic factor; antiangiogenic factor; thrombospondin-1; vascular endothelial growth factor; vascular endothelial growth factor receptor-2

THE RISING INCIDENCE of type 2 diabetes mellitus raises major public health concerns because of the increased risk of cardiovascular complications (1, 2). Diabetic cardiomyopathy (DCM) is defined as left ventricular (LV) dysfunction that occurs independently of coronary artery disease and hypertension (1, 2). Its functional alterations are LV hypertrophy (LVH) and LV diastolic dysfunction, which may precede the development of LV systolic dysfunction (1, 2). Its pathological features involve cardiomyocyte hypertrophy and apoptosis, microvascular pathology, including abnormal capillary density and permeability, and interstitial fibrosis (1, 2, 6).

The activation of the renin-angiotensin system (RAS) is well recognized in DCM. The circulating RAS is downregulated in diabetes (24, 35). Nevertheless, pharmacological blockade of the RAS with ANG II type 1 receptor blockers (ARBs) or angiotensin-converting enzyme inhibitors prevents cardiac damage in diabetic patients (3, 12). Furthermore, ANG II and the other RAS components are elevated in the diabetic heart (5, 6, 46). Therefore, the local RAS, activated in the diabetic heart, independent of the circulating RAS, could induce LV dysfunction and injury through the ANG II type 1 receptor.

Heart ANG II induces LVH by raising blood pressure (40) and acting as a growth factor on cardiomyocytes in the absence of hypertension (23, 41). Cross-talk between cardiomyocytes and the coronary vasculature during cardiac growth is very important in maintaining cardiac function (37, 45). During adaptive cardiac growth, secretion of angiogenic growth factors such as VEGF from hypertrophied cardiomyocytes under chronic hypoxia is responsible for enhanced angiogenesis (37, 45). This, in turn, contributes to cardiac growth and the maintenance of contractile function by carrying O_2 and nutrients into the hypertrophied myocardium (37, 45). However, disruption of the coordination between coronary angiogenesis and cardiac growth results in a transition from adaptive hypertrophy to heart failure with interstitial fibrosis (37, 45). The suppression of angiogenesis associated with cardiac growth is induced by the downregulation of the angiogenic growth factors (37, 45). These reports led us to hypothesize that local ANG II overproduced in the diabetic heart may induce LVH, which may suppress coronary angiogenesis, therefore playing a crucial role in the pathogenesis of DCM. As it stands, direct proof of this hypothesis has been lacking. Furthermore, in the pathogenesis of DCM, it is unclear what factors produced from the hypertrophied cardiomyocytes are involved in the inhibition of coronary angiogenesis.

We used male Spontaneously Diabetic Torii (SDT) rats, a model of human nonobese type 2 diabetes (44), treated with or without the ARB olmesartan medoxomil (Olm) (27) and examined whether and how heart ANG II may disrupt the coordination between LVH and coronary angiogenesis and progress DCM.

Address for reprint requests and other correspondence: S. Muto, Div. of Nephrology, Dept. of Internal Medicine, Jichi Medical Univ., 3311-1 Yakushiji, Shimotsuke, Tochigi 329-0498, Japan (e-mail: smuto@jichi.ac.jp).

MATERIALS AND METHODS

Experimental animals. The study protocol was approved by the Animal Ethics Committee of Jichi Medical University. Male SDT rats and age-matched male Sprague-Dawley rats (both from CLEA Japan, Tokyo, Japan) were housed under specific pathogen-free conditions. The SDT rat used in the present study is an inbred rat strain from an outbred colony of Sprague-Dawley rats (44). Male SDT rats spontaneously develop gradual impairment of insulin secretion and hyperglycemia without obesity after 20 wk of age, with an incidence of 100% at 40 wk of age, but they survive long term without insulin treatment (44). In our study, plasma glucose levels were measured once weekly from 15 wk of age to the onset of diabetes and every 8 wk after that. The onset of diabetes was defined as a plasma glucose concentration >250 mg/dl, as previously described (26). At the onset of diabetes, which we defined as "0 wk," SDT rats were randomly divided into two groups: the SDT group and the Olm-treated group (Olm group). Age-matched male Sprague-Dawley rats were used as a control group. The Olm group was given powdered food (CE-2, CLEA Japan) including a dose [0.01% (wt/wt)] of Olm (Daiichi Sankyo, Tokyo, Japan) (27) for 0, 8, or 16 wk from the onset of diabetes. Both the SDT and control groups were given the powdered food without Olm for the identical three periods. To confirm that the Olm intake was adequate and that the dose of Olm was not toxic, we measured serum Olm concentrations by HPLC (48). Serum Olm concentrations in SDT rats treated with Olm for 8 and 16 wk after the onset of diabetes were 118.4 ± 31.5 ng/ml (n = 5) and 125.8 ± 18.6 ng/ml (n = 5), respectively. These concentrations were not significantly different from each other and corresponded to approximately one-half of the maximum plasma concentration obtained when healthy human volunteers were given a single oral dose of 10-mg Olm (224 ± 45 ng/ml) (42). No serum Olm was detectable in control rats or SDT rats not given Olm.

SDT rats treated with and without Olm at 0, 8, and 16 wk after the onset of diabetes as well as age-matched control rats were killed by decapitation at the corresponding time points. Systolic blood pressure was measured in the conscious state by a noninvasive tail-cuff system (BP-98A, Softron, Tokyo, Japan), as previously described (8, 9, 15). Biochemical and hormonal data from plasma and serum were gathered at SRL (Tokyo, Japan). Immediately after removal, the heart was weighed. Thereafter, LV tissue samples were used for histological analysis, as described below.

Echocardiography. In the three groups of rats at 0, 8, and 16 wk, echocardiographic experiments were performed under 2.5% isoflurane (Dainippon Sumitomo Pharma, Osaka, Japan) anesthesia with an IV-ANE (Olympus, Tokyo, Japan) equipped with a Vevo770 ultrasound biomicroscopy system (VisualSonics, Toronto, ON, Canada) with a 17.5-MHz scan head (RMV 716, VisualSonics) (56). M-mode tracings were recorded through the anterior and posterior LV walls at the papillary muscle level to measure LV end-diastolic dimensions (LVEDD), LV posterior wall thickness (LVPWT), and interventricular septum thickness at end diastole, LV end-systolic dimensions (LVESD) at end systole, and heart rate, as previously described (53). LV fractional shortening (LVFS) was calculated according to the following formula: LVFS (in %) = [(LVEDD − LVESD)/LVEDD] × 100. To assess LV diastolic function, two-dimensional guided Doppler flow measurements of mitral inflow were obtained. Early and late mitral inflow velocity (E-wave and A-wave, respectively) and E-wave deceleration time were measured from the Doppler recordings in the standard fashion, and the *E*-to-*A* ratio (*E*/*A*) was calculated (21).

Histological and morphometric analysis. For paraffin sections, LV tissue samples were fixed in 10% buffered paraformaldehyde and cut into 4-μm cross-sections. For frozen sections, tissue samples were embedded in optimum cutting temperature compound (Sakura Finetek, Tokyo, Japan), frozen in 100% ethanol on dry ice for 30 min, and stored at −80°C, as previously described (43). Frozen tissues were cut into 4-μm cross-sections and stored at −80°C. LV tissues were used for hematoxylin and eosin staining, picro-Sirius red staining, immunohistochemistry, and immunofluorescence. LV tissues stained with the collagen-specific dye picro-Sirius red were used for the quantification of interstitial collagen, as previously described (8, 18). The cardiomyocyte cross-sectional area was determined in LV sections also stained with picro-Sirius red. The cross-sectional area of LV tissues was evaluated throughout the inner third of the LV, as previously described (8). The interstitial collagen volume fraction and cardiomyocyte cross-sectional area were calculated as previously described (8). All histological measurements were carried out using image-analysis software (Image Pro Plus 6.2J, Media Cybernetics, Bethesda, MD), as previously described (8, 15). All quantifications were performed in a blinded manner.

Immunohistochemistry. Immunohistochemistry was performed on formaldehyde-fixed paraffin sections using the Vectastain Elite ABC kit (Vector Laboratories, Burlingame, CA), as previously described (8, 9, 15). The primary antibodies used for the staining were as follows: monoclonal mouse anti-rat endothelial cell antibody (RECA)-1 (1:100, Oxford Biotechnology, Oxford, UK), polyclonal rabbit anti-human von Willebrand factor (vWF) antibody (1:100, Chemicon, Billerica, MA), and monoclonal mouse anti-rat PCNA (1:100, Santa Cruz Biotechnology, Santa Cruz, CA). Negative controls with the same species IgG of each primary antibody and without primary antibody were carefully examined. Slides were viewed with a microscope (BX50, Olympus) equipped with a digital camera (DP71, Olympus), and ≥20 randomly selected LV subendocardial areas (0.141 mm^2/field) were blindly quantified at ×400 magnification using image-analysis software (Image Pro Plus 6.2J, Media Cybernetics) (8, 15).

For capillaries, the number of capillary lumina surrounded by anti-RECA-1-positive or anti-vWF antibody-positive cells with <8-μm lumen size and with 1 nucleus/field was counted, as previously described (15). Capillary density was expressed as the number of capillaries per field. The ratio of the number of capillaries to cardiomyocytes per field (capillary-to-cardiomyocyte ratio) was also determined. To examine whether there was any evidence of capillary endothelial cell proliferation, double immunostaining was performed with anti-RECA-1 and anti-PCNA antibodies, as previously described (15). For proliferative capillaries, the numbers of proliferative capillaries (anti-RECA-1-positive and anti-PCNA-positive cells) and all capillaries (anti-RECA-1-positive cells) were counted per LV field, and the percentage of proliferative capillaries was expressed as the percentage of proliferative capillaries compared with the total number of capillaries.

Identification of apoptosis. Apoptotic cells, including cardiomyocytes and capillary endothelial cells, were identified based on the presence of fragmented nuclear DNA in histological sections labeled using the terminal deoxynucleotidyl transferase dUTP nick-end labeling (TUNEL) method, as previously described (15, 19).

Capillary endothelial cell apoptosis was identified by double labeling using TUNEL and anti-RECA-1, as previously described (15). Slides were viewed with a microscope (BX50, Olympus) equipped with a digital camera (DP71, Olympus), and ≥20 randomly selected LV areas (0.141 mm^2/field) were blindly quantified at ×400 magnification using image-analysis software (Image Pro Plus 6.2J, Media Cybernetics), as previously described (8, 15). For apoptotic capillaries, the numbers of apoptotic capillaries (anti-RECA-1-positive and TUNEL-positive cells) and all capillaries (anti-RECA-1-positive cells) per LV field were counted, and the percentage of apoptotic capillaries was calculated out of the total number of capillaries.

Immunofluorescence. Immunofluorescence staining for ANG II and cardiac myosin in the LV was performed using frozen sections; staining for other proteins in the LV was carried out using formaldehyde-fixed paraffin sections. The tissue was permeabilized using 1% Triton X-100 (10 min, room temperature). Nonspecific binding was blocked using 2% BSA plus 5% normal goat serum. The primary antibodies used for the staining were as follows: polyclonal goat

anti-ANG II (1:200, Santa Cruz Biotechnology), monoclonal mouse anti-hypoxia-inducible factor (HIF)-1α (1:500, Chemicon), affinity purified rabbit anti-VEGF (1:200, Immuno-Biological Laboratories, Gunma, Japan), monoclonal mouse anti-thrombospondin (TSP)-1 (1:50, Santa Cruz Biotechnology), monoclonal mouse anti-heavy chain cardiac myosin (1:100, Abcam, Cambridge, MA), and monoclonal mouse anti-RECA-1 (1:100, Oxford Biotechnology). For quantification of the expression of ANG II in LV tissues, the fluorescence intensity was measured in more than five randomly selected areas of the stained tissue within a given field using a computerized image-analysis system (Image Pro Plus 6.2J, Media Cybernetics), as previously described (43). Expression of ANG II, VEGF, and TSP-1 in SDT rat LV tissues was also performed using double staining with antibodies against each plus cardiac myosin. The percentage of particles expressed in cardiomyocytes was calculated using 500 randomly selected particles. Expression of HIF-1α in cardiomyocytes was measured using triple staining with antibodies against cardiac myosin, HIF-1α, and 4′,6-diamidino-2-phenylindole (a stain for nuclei). The percentage of HIF-1α-positive nuclei was calculated using 1,000 randomly selected nuclei in each group. The fluorescence signal was visualized with a fluorescence microscope equipped with a fluorescein isothiocyanate filter (AX80, Olympus) and was quantified with image-analysis software (Image Pro Plus 6.2J, Media Cybernetics), as previously described (8, 15).

Serum ANG II and local ANG II in the LV. Levels of serum and LV ANG II were measured by RIA (SRL), as previously described (50). LV ANG II levels were normalized for protein content by the Biuret method, measured in the same samples.

Western blot analysis. LVs were homogenized in RIPA buffer (150 mM NaCl, 50 mM Tris·HCl, 0.5% Nonidet P-40, and 0.1% SDS) containing protease inhibitors (Complete Mini, Roche, Mannheim, Germany). Lysates were then centrifuged for 40 min at 14,000 rpm at 4°C. Protein concentrations were determined using BCA Protein Assay Reagent (Thermo Fisher Scientific, Kanagawa, Japan). Ten micrograms of protein were separated by SDS-PAGE (4–12% NuPAGE Novex Bis Tris Gel, Invitrogen, Carlsbad, CA) followed by transfer to a polyvinylidene difluoride membrane (Hybond-P, GE Healthcare, Little Chalfont, UK). The primary antibodies used for Western blot analysis were as follows: polyclonal rabbit anti-EGF receptor (EGFR; 1:200, Santa Cruz Biotechnology), monoclonal mouse anti-phosphorylated EGFR (pEGFR) at Tyr^{1173} (1:100, Santa Cruz Biotechnology), polyclonal rabbit anti-Na^+/H^+ exchanger isoform 1 (NHE1; 1:200, Chemicon), polyclonal goat anti-human transforming growth factor (TGF)-β_1 (1:200, Santa Cruz Biotechnology), affinity-purified anti-VEGF (1:200, Immuno-Biological Laboratories), monoclonal mouse anti-TSP-1 (1:50, Santa Cruz Biotechnology), polyclonal rabbit anti-phosphorylated Flk-1 [phosphorylated VEGF receptor-2 (pVEGFR2)] at Tyr^{1214} (1:200, Santa Cruz Biotechnology), and monoclonal mouse anti-β-actin (1:2,000, Santa Cruz Biotechnology). Bands were detected by enhanced chemiluminescence (GE Healthcare). Membranes were reblotted with anti-β-actin antibody as a loading control. The signal band density was quantified using ImageJ (version 1.63, National Institutes of Health, http://rsb.info.nih.gov/nih-image/) and was normalized to that of the corresponding β-actin band.

Statistical analyses. Results are presented as means ± SE. Data were analyzed using paired or unpaired Student's *t*-tests for comparisons of parameters between two groups or ANOVA for comparisons of parameters among three groups, followed by post hoc analysis with the Fisher test, where appropriate. *P* values of <0.05 were considered statistically significant.

RESULTS

Characteristics of SDT rats as a model of human nonobese type 2 diabetes. Diabetes onset in male SDT rats varied from 17 to 32 wk of age, as previously reported (22, 44). Unlike other studies (7, 25), which used age-matched male SDT rats with different diabetes onsets and durations, we used male SDT rats with the same diabetes onsets and durations and characterized their diabetic features at 0, 8, and 16 wk after diabetes onset. At 0 wk, the ages of the control, SDT, and Olm groups of rats used in the study were 22.7 ± 1.1, 22.2 ± 0.7, and 22.6 ± 0.7 wk (n = 25 rats/group), respectively; this did not differ statistically among the groups. Food intake in both SDT and control rats increased with time; the magnitude was greater in SDT rats at 0, 8, and 16 wk (Fig. 1*A*). Nonetheless, the body weight of SDT rats was almost identical to that of control rats at 0 wk but decreased at 8 and 16 wk, although the body weight of control rats gradually increased with time (Fig.

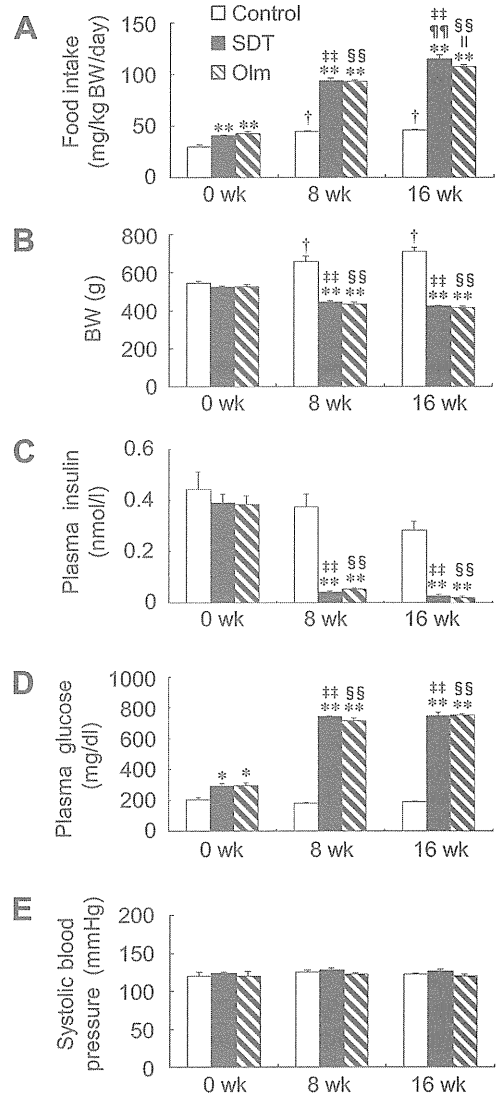

Fig. 1. Clinical features of spontaneously diabetic Torii (SDT) rats as a model of human nonobese type 2 diabetes. *A–E*: food intake (*A*), body weight (BW; *B*), plasma insulin (*C*), plasma glucose (*D*), and systolic blood pressure (*E*) in SDT rats without (SDT group) and with olmesartan medoxomil (Olm group) at 0, 8, and 16 wk after the onset of diabetes as well as age-matched control rats (control group) at the corresponding time points. Data are means ± SE of 5–7 rats/group. $*P < 0.05$ and $**P < 0.001$ vs. the control group at the same time point; $\dagger P < 0.05$ vs. the 0-wk control group; $\ddagger\ddagger P < 0.001$ vs. the 0-wk SDT group; $\S\S P < 0.001$ vs. the 0-wk Olm group; $\P\P P < 0.001$ vs. the 8-wk SDT group; $\| P < 0.001$ vs. the 8-wk Olm group.

1*B*). Insulin secretion in SDT rats was nearly identical to that of control rats at 0 wk but decreased at 8 and 16 wk (Fig. 1*C*). Plasma glucose in SDT rats was already greater than in control rats at 0 wk, despite similar plasma insulin levels, and increased further at 8 and 16 wk (Fig. 1*D*). Systolic blood pressure did not differ between the groups (Fig. 1*E*). Therefore, SDT rats can be used as a model of human nonobese type 2 diabetes, characterized by insulin resistance at diabetes onset, impaired insulin secretion at 8 and 16 wk, but no systolic blood pressure elevation. These parameters were unaffected by Olm (Fig. 1, *A–E*).

LV function and dimensions in SDT rats. LV diastolic function was impaired in SDT rats at 8 and 16 wk; they exhibited an increase in deceleration time, with the degree of increase being greater at 16 wk (Fig. 2, *A* and *B*). SDT rats also exhibited a decrease in *E*/*A* at 16 wk only (Fig. 2, *A* and *C*). LV systolic function assessed by LVFS was preserved in SDT rats at 8 wk but was impaired at 16 wk (Fig. 2*D*). Because brain natriuretic peptide levels were not elevated, no heart failure was observed in SDT rats (data not shown). LVH, as demonstrated by an increase in LVPWT (Fig. 2*E*), was evident in SDT rats at 8 and 16 wk. Olm treatment reversed these abnormalities in SDT rats (Fig. 2, *A–E*). In control rats, LVPWT was greater at 16 wk than at 0 wk (Fig. 2*E*). Heart rate or interventricular septum thickness did not differ among the groups (data not shown). Thus, SDT rats after diabetes onset developed LV diastolic dysfunction at 8 wk, followed by moderate LV systolic dysfunction at 16 wk, similar to the pattern observed in human DCM (1, 2), and LVH at 8 and 16 wk.

Cardiomyocyte hypertrophy and interstitial fibrosis in SDT rats. Because LVH includes cardiomyocyte growth (hypertrophy) and/or extracellular matrix accumulation, we measured the cross-sectional area of single cardiomyocytes and the interstitial collagen volume fraction in LVs stained by picro-Sirius red. In SDT rat LVs, single cardiomyocyte cross-sectional areas were increased at 8 and 16 wk compared with those in control rats, with a greater degree at 16 wk (Fig. 3, *A* and *B*). The interstitial collagen volume fraction was increased at 16 wk only (Fig. 3, *A* and *C*). Both were completely normalized by Olm (Fig. 3, *A–C*). Thus, SDT rats after diabetes onset developed cardiomyocyte hypertrophy at 8 wk, followed by interstitial fibrosis at 16 wk; both were Olm sensitive. On the other hand, similar to the change in LVPWT, single cardiomyocyte cross-sectional areas in control rats were greater at 16 wk than at 0 wk (Fig. 3*B*), suggesting a possibility that these may be age-associated changes (13, 51).

LV ANG II in SDT rats. Circulating and cardiac ANG II induce cardiac hypertrophy and fibrosis in hypertensive and normotensive animals (16, 23, 36, 40, 52). It has been reported that heart ANG II induces cardiac hypertrophy and fibrosis in diabetic patients (6) and streptozotocin-induced (STZ) diabetic rats (5). Thus, we measured the concentrations of serum and LV ANG II. At 8 and 16 wk, but not at 0 wk, serum ANG II levels were lower in SDT rats than in control rats, but both LV tissue ANG II levels and LV tissue immunofluorescence intensity were greater in SDT rats; all of these were completely reversed by Olm (Fig. 4, *A–C*). Almost all (99.6%) ANG II-positive particles colocalized with cardiac myosin, a cardiomyocyte marker, in the SDT rat LV at 16 wk (Fig. 4*D*). Therefore, local ANG II was overproduced by SDT rat LV

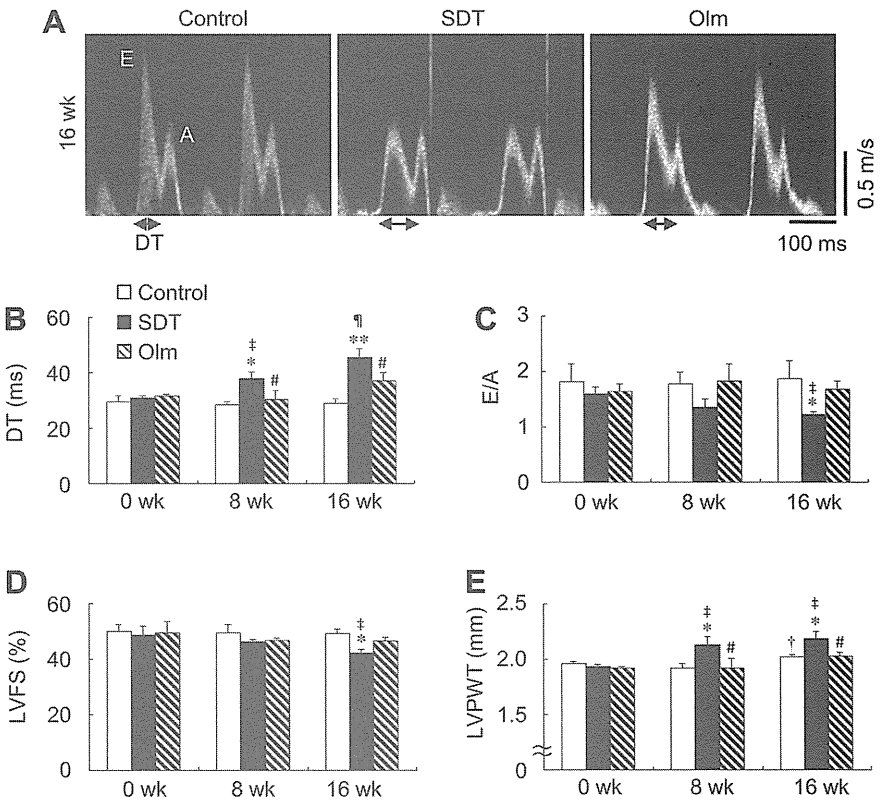

Fig. 2. Echocardiographic findings in the three groups of rats. *A*: representative Doppler flow measurements of mitral inflow obtained from the three groups of rats at 16 wk. DT, deceleration time; E, E-wave; A, A-wave. *B–E*: E-wave DT (*B*), E-wave-to-A-wave ratio (*E*/*A*; *C*), left ventricular (LV) fractional shortening (LVFS; *D*), and LV posterior wall thickness (LVPWT; *E*) in the three groups of rats at 0, 8, and 16 wk. Data are means ± SE of 5–7 rats/group. $*P < 0.05$ and $**P < 0.001$ vs. the control group at the same time point; $\#P < 0.05$ vs. the SDT group at the same time point; $\dagger P < 0.05$ vs. the 0-wk control group, $\ddagger P < 0.05$ vs. the 0-wk SDT group; $\P P < 0.05$ vs. the 8-wk SDT group.

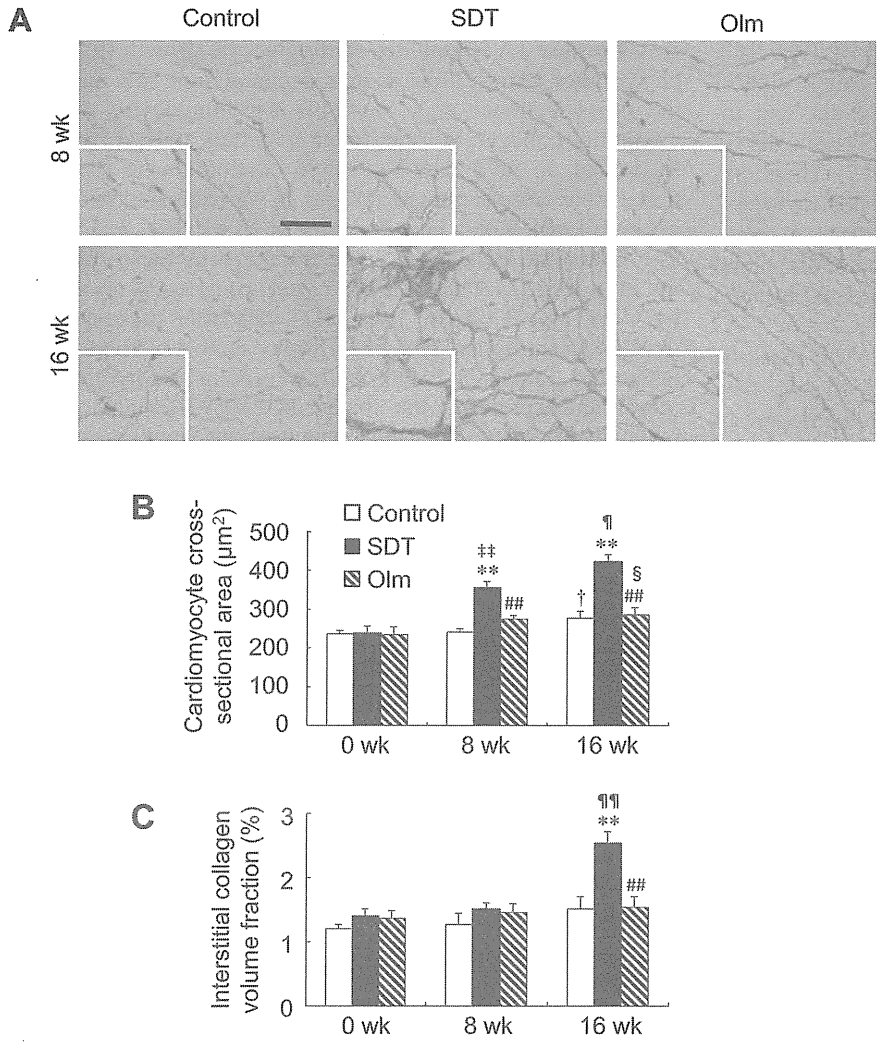

Fig. 3. Cardiomyocyte cross-sectional area and interstitial collagen volume fraction in the three groups of rats. *A*: representative micrographs of picrosirius red staining in the three groups of rats at 8 and 16 wk. Typical cardiomyocytes are shown in the higher-magnification boxes. Scale bar = 100 μm. *B* and *C*: cardiomyocyte cross-sectional area (*B*) and interstitial collagen volume fraction (*C*) by picrosirius red staining in the three groups of rat LVs at 0, 8, and 16 wk. Data are means ± SE of 6–7 rats/group. $^{**}P < 0.001$ vs. the control group at the same time point; $^{\#\#}P < 0.001$ vs. the SDT group at the same time point; $^{\dagger}P < 0.05$ vs. the 0-wk control group; $^{\ddagger\ddagger}P < 0.001$ vs. the 0-wk SDT group; $^{\P}P < 0.05$ and $^{\P\P}P < 0.001$ vs. the 8-wk SDT group; $^{\S}P < 0.05$ vs. the 0-wk Olm group.

cardiomyocytes at 8 and 16 wk, and this was completely reversed by Olm. These findings indicate that local ANG II overproduced in SDT rat LV cardiomyocytes induced both cardiomyocyte hypertrophy at 8 and 16 wk and interstitial fibrosis at 16 wk.

Factors involved in cardiomyocyte hypertrophy and interstitial fibrosis in SDT rats. Because EGFR transactivation (49) and NHE1 activation (4) are important downstream signals for ANG II-induced LVH, we next examined the expression of pEGFR, total EGFR, and NHE1 in the LV. At 8 and 16 wk, there were increased protein levels of pEGFR and NHE1 in SDT rats, both of which were completely suppressed by Olm, although the expression of total EGFR did not differ among the groups (Fig. 5, *A* and *B*). Thus, these findings indicate that both enhanced EGFR phosphorylation and NHE1 upregulation were involved in the local ANG II-induced cardiomyocyte hypertrophy in SDT rats at 8 and 16 wk.

The profibrotic growth factor TGF-β_1 plays an important role in cardiac fibrosis, and ANG II is known to enhance TGF-β_1 expression in the myocardium (52). Moreover, ANG II infusion in mice enhances cardiomyocyte apoptosis (16). Thus, we examined the expression of TGF-β_1 and measured the number of TUNEL-positive cardiomyocytes in LV tissues. In conjunction with interstitial fibrosis in the LV tissue, the SDT rat LV tissue at 16 wk alone exhibited increases in TGF-β_1 expression and in the number of TUNEL-positive cardiomyocytes, both of which were completely reversed by Olm (Fig. 5, *C* and *D*). Therefore, these results suggest that both TGF-β_1 upregulation and cardiomyocyte apoptosis may contribute to the local ANG II-induced interstitial fibrosis in the SDT rat LV tissue at 16 wk only.

Coronary capillary angiogenesis associated with cardiomyocyte hypertrophy in SDT rats. To test whether the LV ANG II-induced cardiomyocyte hypertrophy in SDT rats at 8 and 16 wk affects coronary capillary angiogenesis, we examined the capillary density and capillary-to-cardiomyocyte ratio by staining endothelial cells with anti-RECA-1. We found that in SDT rats, both capillary density and the capillary-to-cardiomyocyte ratio increased at 8 wk but conversely decreased at 16 wk; both were completely reversed by Olm (Fig. 6, *A–C*). By labeling with a second endothelial cell marker (anti-vWF antibody), similar changes in the microvasculature were observed (data not shown). Thus, in SDT rat LVs after the onset of diabetes, coronary capillary angiogenesis associated with LV ANG II-induced cardiomyocyte hypertrophy was enhanced at 8 wk but was suppressed at 16 wk.

We next examined whether either the proliferation and/or apoptosis of capillary endothelial cells contribute to the

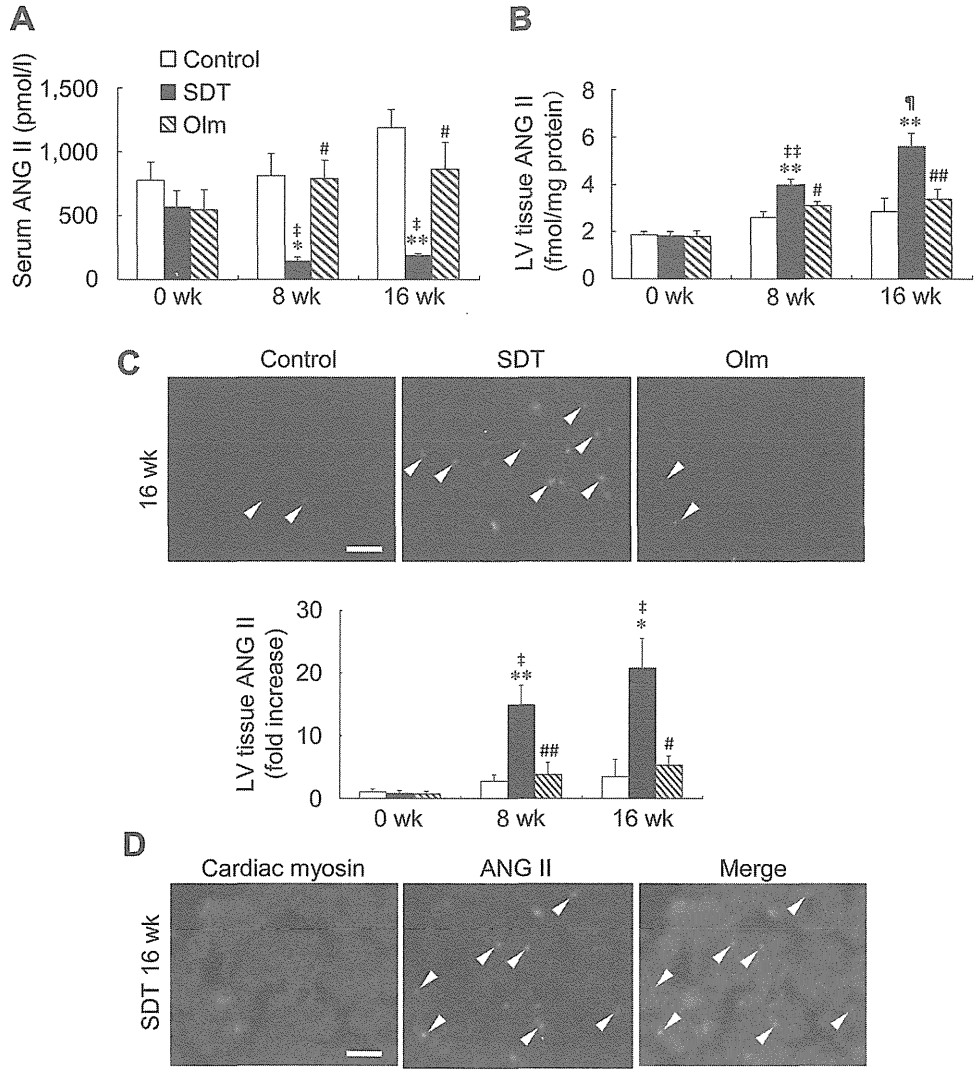

Fig. 4. Serum and LV tissue ANG II in the three groups of rats. *A* and *B*: serum ANG II (*A*) and LV ANG II (*B*) in the three groups of rats at 0, 8, and 16 wk. Data are means ± SE of 7 rats/group. *C*, *top*: representative ANG II immunofluorescence images in the three groups of rat LV tissues at 16 wk. Arrowheads show ANG II-expressing particles. Scale bar = 20 μm. *Bottom*, densitometric analyses of LV ANG II immunofluorescence intensity relative to that in the control group at 0 wk. Data are means ± SE of 5 rats/group. *D*: representative immunofluorescence double staining for cardiac myosin (a cardiomyocyte marker) and ANG II in the LV of the SDT group at 16 wk. Arrowheads show ANG II expressed in cardiomyocytes. Scale bar = 20 μm. $*P < 0.05$ and $**P < 0.001$ vs. the control group at the same time point; $\#P < 0.05$ and $\#\#P < 0.001$ vs. the SDT group at the same time point; $\ddagger P < 0.05$ and $\ddagger\ddagger P < 0.001$ vs. the 0-wk SDT group; $\P P < 0.05$ vs. the 8-wk SDT group.

coronary angiogenesis associated with the LV ANG II-induced cardiomyocyte hypertrophy at 8 and 16 wk. In SDT rat LVs, the percentages of PCNA-positive capillaries and TUNEL-positive capillaries increased at 8 and 16 wk, respectively, and these increases were completely reversed by Olm (Fig. 7, *A* and *B*). On the other hand, the percentages of TUNEL-positive capillaries and PCNA-positive capillaries in SDT rat LVs were unchanged at 8 and 16 wk, respectively (Fig. 7, *A* and *B*).

Chronic hypoxia in hypertrophied cardiomyocytes is a trigger for coronary capillary angiogenesis in SDT rats at 8 wk. HIF-1α is a key transcription factor for the hypoxic induction of angiogenic growth factors, such as VEGF. To test whether chronic hypoxia in hypertrophied cardiomyocytes is a trigger for coronary capillary angiogenesis, we examined the expression of the two hypoxia-responsive proteins: HIF-1α and VEGF. In accordance with the degree of cardiomyocyte hypertrophy, the percentage of HIF-1α-positive nuclei in SDT rat LV cardiomyocytes increased at 8 and 16 wk, with a higher percentage at 16 wk (Fig. 8*A*). VEGF expression in the LV was also upregulated in SDT rats at 8 and 16 wk (Fig. 8*B*). Almost all (97.1%) of VEGF-positive particles colocalized with cardiac myosin in the SDT rat LV at 16 wk (Fig. 8*C*). The upregulation of HIF-1α and VEGF was completely abolished by Olm (Fig. 8, *A* and *B*). Therefore, hypertrophied cardiomyocytes in SDT rat LVs at 8 and 16 wk were subjected to chronic hypoxia that was completely reversed by Olm.

VEGF possesses angiogenic activity through binding to its tyrosine kinase receptors, including VEGFR2, which is expressed almost exclusively in endothelial cells (31), and thereafter through pathways involving their phosphorylation (33). Thus, we next examined whether VEGFR2 phosphorylation is involved in the coronary angiogenesis associated with cardiomyocyte hypertrophy in SDT rat LVs at 8 and 16 wk. In parallel with the upregulation of VEGF in SDT rat LV cardiomyocytes at 8 wk, there were increased protein levels of pVEGFR2 compared with those in control cardiomyocytes, which were completely normalized by Olm (Fig. 8*D*). In contrast, at 16 wk, despite the upregulation of VEGF in SDT rat LV cardiomyocytes, the protein levels of pVEGFR2 were not increased significantly compared with those in control cardiomyocytes (Fig. 8*D*). These findings indicate that, in SDT rat LVs, VEGF produced from hypertrophied cardiomyocytes under chronic hypoxia and

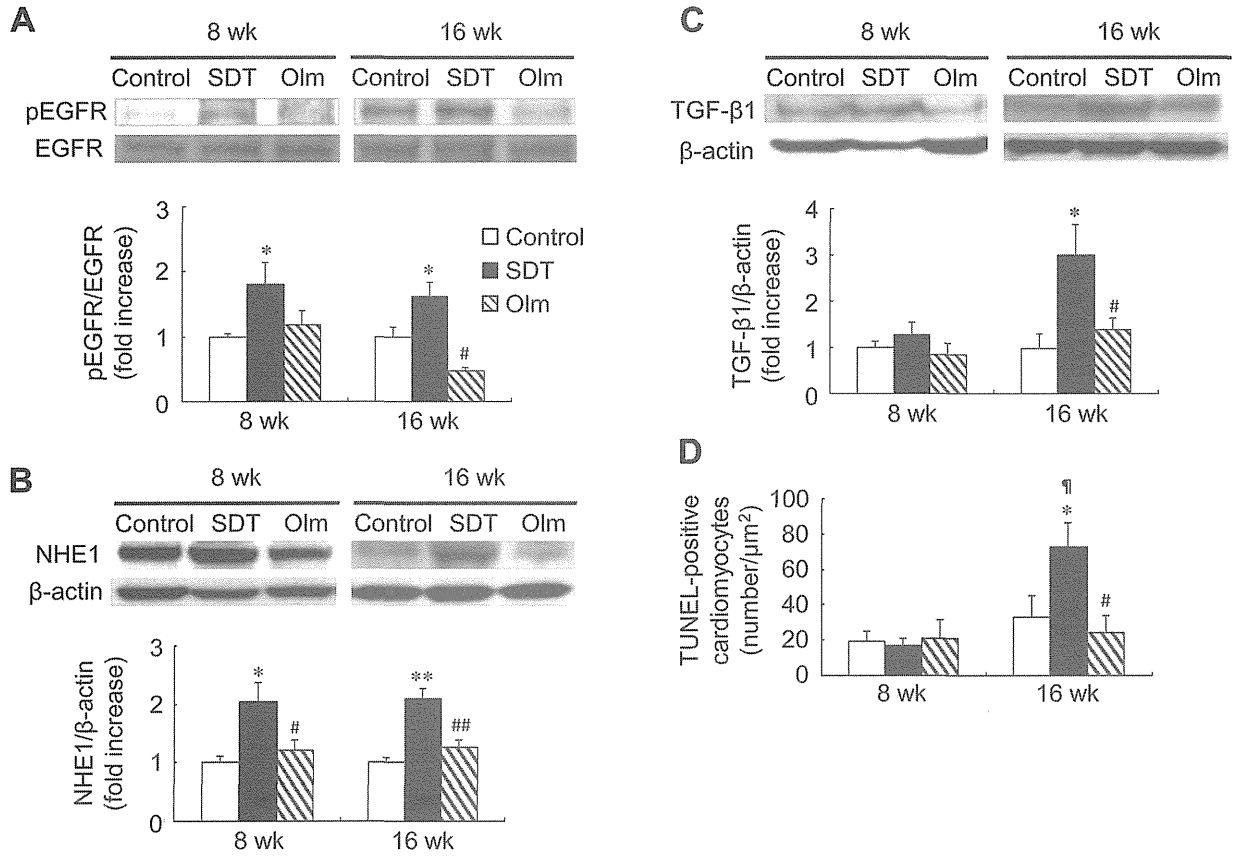

Fig. 5. Factors involved in cardiomyocyte hypertrophy and interstitial fibrosis in SDT rats. *A–C*, *top*: Western blot analyses of EGF receptor (EGFR) and phosphorylated EGFR (pEGFR) (*A*), Na^+/H^+ exchanger isoform 1 (NHE1; *B*), and transforming growth factor (TGF)-β_1 (*C*) in the three groups of rat LV tissues at 8 and 16 wk. Data are means ± SE of 4–5 rats/group. *Bottom*, densitometric analyses of the expression of pEGFR relative to EGFR (*A*) and the expression of each protein (*B* and *C*) in the three groups of rats at 8 and 16 wk compared with the control group at 8 and 16 wk, respectively. *D*: terminal deoxynucleotidyl transferase dUTP nick-end labeling (TUNEL)-positive cardiomyocytes in the three groups of rat LV tissues at 8 and 16 wk. Data are means ± SE of 5 rats/group. $*P < 0.05$ and $**P < 0.001$ vs. the control group at the same time point; $\#P < 0.05$ and $\#\#P < 0.001$ vs. the SDT group at the same time point; $\P P < 0.05$ vs. the 8-wk SDT group.

VEGFR2 phosphorylation contribute to the increased coronary angiogenesis at 8 wk only.

Mechanisms of suppression of coronary angiogenesis associated with cardiomyocyte hypertrophy in SDT rats at 16 wk. The above finding, that the angiogenesis in SDT rats at 16 wk was suppressed despite the upregulation of the angiogenic factor VEGF, suggests the possibility that antiangiogenic factors may overcome the stimulatory effects of VEGF on coronary angiogenesis. To test this, we examined the expression of TSP-1 in the LV tissue, because TSP-1 inhibits angiogenesis by inducing endothelial cell apoptosis (10, 17) and suppressing endothelial cell proliferation (14). At 16 wk alone, expression of TSP-1 in LVs was upregulated in SDT rats and could be completely suppressed by Olm (Fig. 9, *A* and *B*). Notably, almost all (92.2%) TSP-1-positive particles colocalized with cardiac myosin in the SDT rat LV at 16 wk (Fig. 9*C*). These results indicate that, in SDT rat LVs, TSP-1 produced from hypertrophied cardiomyocytes under chronic hypoxia is involved in the reduced coronary angiogenesis at 16 wk only.

DISCUSSION

Using functional and morphological investigation of SDT rats for 16 wk after the onset of diabetes, we focused on the cross-talk between cardiomyocytes and the coronary vasculature during cardiac growth and analyzed the pathogenesis of DCM that mimics human type 2 diabetes.

SDT rats at 8 wk exhibited LVH because of LV cardiomyocyte hypertrophy, and this was accompanied by moderate LV diastolic dysfunction. Since the hypoxia-responsive transcription factor HIF-1α was upregulated in SDT rat LV cardiomyocytes at 8 wk, the hypertrophied cardiomyocytes were under chronic hypoxia, which triggered VEGF production in the cardiomyocytes. This promoted coronary angiogenesis by enhancing capillary endothelial cell proliferation via VEGFR2 phosphorylation, leading to an increase in the capillary-to-cardiomyocyte ratio. Therefore, SDT rats at 8 wk showed an early adaptive phase with coordinated coronary capillary angiogenesis and cardiomyocyte hypertrophy. Similarly, coordinated coronary angiogenesis associated with cardiac hypertrophy has been described in the acute phase in mice after Akt transgene induction (45) and in the early adaptive phase in mice receiving a severe transverse aorta constriction (37). In these animals, coronary angiogenesis was also induced by the upregulation of hypoxia-induced angiogenic factors, including VEGF, expressed in their hearts (37, 45).

In SDT rat LVs at 16 wk, in addition to sustained cardiomyocyte hypertrophy, interstitial fibrosis with cardiomyocyte apoptosis and TGF-β_1 upregulation was observed, and this was

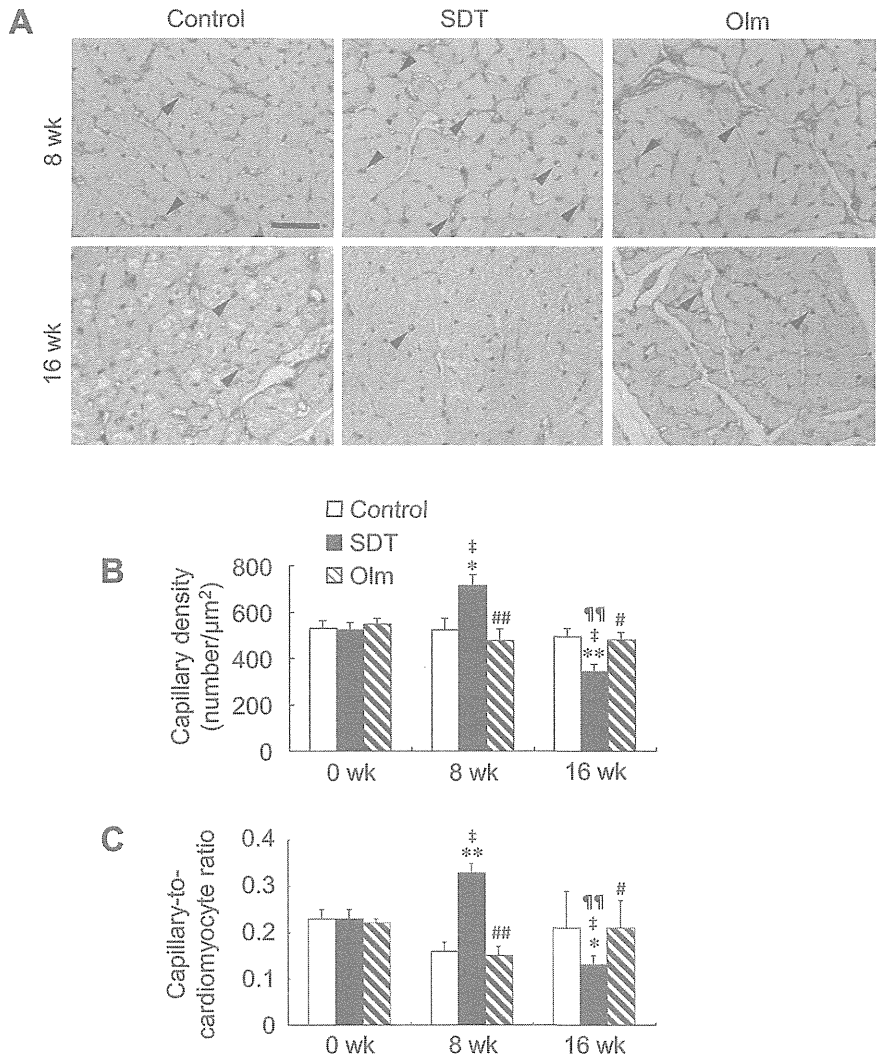

Fig. 6. Coronary capillary angiogenesis associated with cardiomyocyte hypertrophy in SDT rats. *A*: representative micrographs of immunostaining of endothelial cells with anti-rat endothelial cell antibody (RECA)-1 in the three groups of rat LV tissues at 8 and 16 wk. Arrowheads show anti-RECA-1-positive capillaries. Scale bar = 50 μm. *B* and *C*: capillary density (*B*) and the capillary-to-cardiomyocyte ratio (*C*) in the three groups of rat LVs at 0, 8, and 16 wk. Data are means ± SE of 5–7 rats/group. $*P < 0.05$ and $**P < 0.001$ vs. the control group at the same time point; $\#P < 0.05$ and $\#\#P < 0.001$ vs. the SDT group at the same time point; $‡P < 0.05$ vs. the 0-wk SDT group; ¶¶$P < 0.001$ vs. the 8-wk SDT group.

accompanied by progressive LV diastolic dysfunction and moderate LV systolic dysfunction. Furthermore, the degree of cardiomyocyte hypertrophy was significantly greater at 16 wk. The degree of chronic hypoxia in hypertrophied cardiomyocytes was also significantly greater at 16 wk, because the upregulation of HIF-1α in cardiomyocytes was greater at 16 wk than at 8 wk. Moreover, in accordance with HIF-1α upregulation, the upregulated VEGF was maintained. Nevertheless, the SDT rat LV at 16 wk showed the suppression of coronary capillary angiogenesis, resulting in a decrease in the capillary-to-cardiomyocyte ratio. This led to deteriorating chronic hypoxia in extensively hypertrophied cardiomyocytes and therefore to cardiomyocyte apoptosis and consequently to the development of interstitial fibrosis. Therefore, SDT rats at 16 wk represented a maladaptive late phase with a loss of coordination between coronary angiogenesis and cardiomyocyte hypertrophy. Also in the chronic phase in the mice mentioned above (37, 45), coronary angiogenesis associated with cardiomyocyte hypertrophy was inhibited, and the loss of coordinated coronary angiogenesis with cardiomyocyte hypertrophy progressed from adaptive cardiac hypertrophy to heart failure. In the chronic phase in these animals, downregulation of VEGF led to impaired coronary angiogenesis and contractile dysfunction without changing the expression of antiangiogenic factors such as TSP-1. In sharp contrast to these reports, in the late phase of our diabetic model, we observed TSP-1 upregulation in extensively hypertrophied cardiomyocytes with increased capillary endothelial cell apoptosis and reduced capillary endothelial cell proliferation. Furthermore, VEGFR2 phosphorylation was not increased. Similarly, in diabetic Zucker rats, increased expression of TSP-1 in the adventitia of the aorta and a reduced number of vasa vasorum in the aorta have been reported, and a potent antiangiogenic effect of TSP-1 on the vasa vasorum has been suggested (47). TSP-1, a 450-kDa glycoprotein secreted into the extracellular matrix by many cell types, is a naturally occurring antiangiogenic factor (10, 14, 19). It has been reported that TSP-1 inhibits angiogenesis by inducing endothelial cell apoptosis (10, 19) and suppressing endothelial cell proliferation (14). Our laboratory (15) previously reported in the kidney cortex of DOCA/salt hypertensive rats that the upregulation of TSP-1 in their cortical tubule cells occurred despite the upregulation of HIF-1α and VEGF, and this led to peritubular capillary loss and the development of tubulointerstitial fibrosis. Kaur et al. (20) recently reported that TSP-1 inhibited VEGF-stimulated VEGFR2 phosphorylation and its downstream signaling in

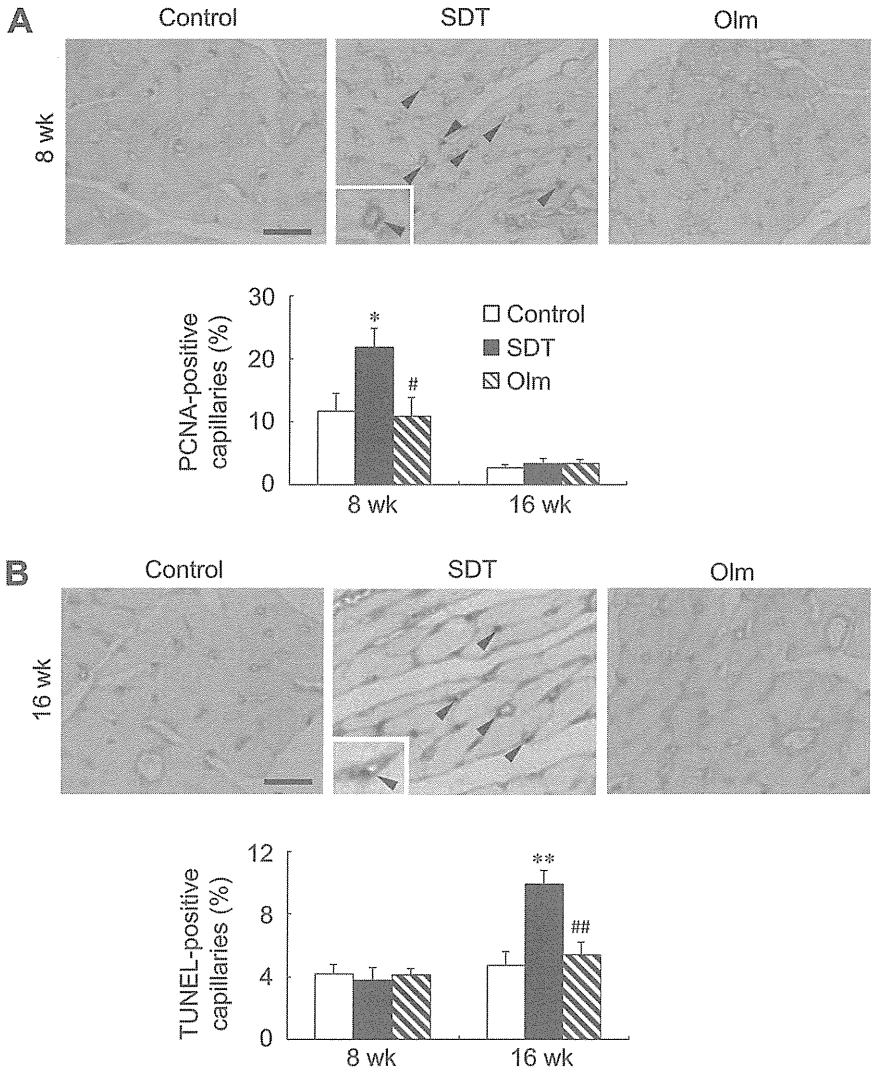

Fig. 7. PCNA-positive capillaries and TUNEL-positive capillaries in the three groups of rat LVs. *A*, *top*: representative micrographs of proliferating capillary endothelial cells (arrowheads) double labeled with anti-PCNA (black) and anti-RECA-1 (brown) in the three groups of rat LV tissues at 8 wk. A typical PCNA-positive capillary endothelial cell is shown expanded in the *inset*. Scale bar = 30 μm. *Bottom*, PCNA-positive capillaries in the three groups of rat LVs at 8 and 16 wk. Data are means ± SE of 5–7 rats/group. *B*, *top*: representative micrographs of apoptotic capillary endothelial cells (arrowheads) double labeled by TUNEL (black) and anti-RECA-1 (brown) in the three groups of rat LV tissues at 16 wk. A typical TUNEL-positive capillary endothelial cell is shown expanded in the *inset*. Scale bar = 30 μm. *Bottom*, TUNEL-positive capillaries in the three groups of rat LVs at 8 and 16 wk. Data are means ± SE of 5–7 rats/group. $*P < 0.05$ and $**P < 0.001$ vs. the control group at the same time point; $\#P < 0.05$ and $\#\#P < 0.001$ vs. the SDT group at the same time point.

cultured endothelial cells, although TSP-1 alone had no effect on VEGFR2 phosphorylation or its downstream signaling. Accordingly, TSP-1 upregulated in the extensively hypertrophied cardiomyocytes of SDT rat LVs at 16 wk could both induce capillary endothelial cell apoptosis and suppress capillary endothelial cell proliferation via the inhibition of VEGF-stimulated VEGFR2 phosphorylation and thereby overcome the stimulatory effect of VEGF on coronary angiogenesis, leading to coronary capillary loss. These findings are compatible with those in a recent study (28) showing that in cultured human microvascular endothelial cells, despite the induction of VEGF in hypoxia-conditioned media, the increased levels of TSP-1 were able to override the protective effects of VEGF on their survival and proliferation. Taking these previous reports together with our findings, the signals from the hypertrophied cardiomyocytes under chronic hypoxia to inhibit coronary angiogenesis differ markedly between the above-mentioned models (37, 45) and our own, and we suggest an important role for TSP-1 as an antiangiogenic factor in the diabetic heart of SDT rats.

Our findings that, in SDT rat LVs at 16 wk, the expression of VEGF protein was upregulated but VEGFR2 phosphorylation did not increase, are consistent with those obtained from diabetic patients (39) and rats (38). Sasso et al. (39) showed that type 2 diabetic patients with chronic coronary heart disease had significantly higher myocardial VEGF mRNA and protein levels and lower VEGFR2 mRNA and protein levels than nondiabetic subjects, along with a downregulation of VEGF-dependent intracellular signaling, including reduced VEGFR2 phosphorylation. It has been reported that, in STZ diabetic rat hearts 90 days after the induction of diabetes, the expression of VEGF mRNA was increased, but the expression of VEGFR2 mRNA was unaffected (38). These two reports proposed several potential mechanisms for their observations but did not investigate the relationship between the expression of VEGF and its downstream signaling, coronary capillary angiogenesis associated with cardiomyocyte hypertrophy, and cardiac function. The present study represents a novel mechanism responsible for their observations. In sharp contrast to the data from STZ diabetic rats mentioned above (38), Yoon et al. (54) performed serial clinicopathological investigation of STZ diabetic rats over 1 yr and reported that a progressive decrease of myocardial VEGF expression was the initial event, followed by reduced coronary capillary angiogenesis with decreased phosphorylation of VEGFR2 and increased capillary endothelial cell apoptosis, resulting in the progression of DCM with

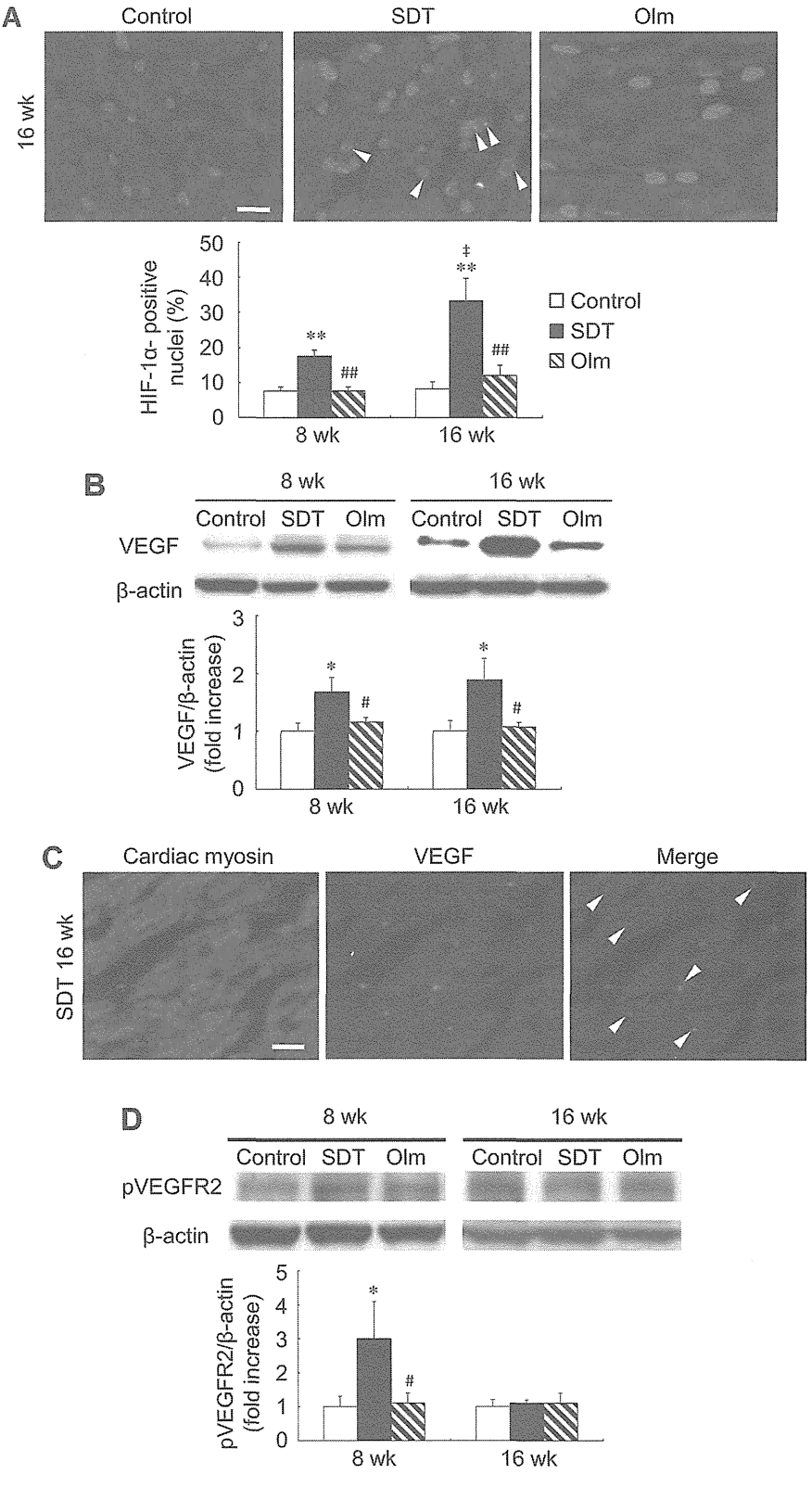

Fig. 8. Expression of hypoxia-inducible factor (HIF)-1α, VEGF, and phosphorylated VEGF receptor-2 (pVEGFR2) in the three groups of rat LVs. *A*, *top*: immunofluorescence triple staining for cardiac myosin, HIF-1α, and 4′,6-diamidino-2-phenylindole (DAPI) in the three groups of rat LVs. Arrowheads show HIF-1α-positive nuclei expressed in cardiomyocytes. Scale bar = 20 μm. *Bottom*, summary of HIF-1α-positive nuclei in the three groups of rat LVs. Data are means ± SE of 6 rats/group. *B*, *top*: Western blot analyses of VEGF in the three groups of rat LV tissues at 8 and 16 wk. *Bottom*, densitometric analyses of the expression of VEGF protein in the three groups of rats at 8 and 16 wk relative to that in the control group at 8 and 16 wk, respectively. Data are means ± SE of 6 rats/group. *C*: immunofluorescence double staining for cardiac myosin and VEGF in the LV tissue of the SDT group at 16 wk. Arrowheads show VEGF expressed in cardiomyocytes. Scale bar = 20 μm. *D*, *top*: Western blot analyses of pVEGFR2 in the three groups of rat LV tissues at 8 and 16 wk. *Bottom*, densitometric analyses of the expression of pVEGFR2 in the three groups of rats at 8 and 16 wk relative to that in the control group at 8 and 16 wk, respectively. Data are means ± SE of 6 rats/group. $*P < 0.05$ and $**P < 0.001$ vs. the control group at the same time point; $\#P < 0.05$ and $\#\#P < 0.001$ vs. the SDT group at the same time point; $‡P < 0.05$ vs. the 8-wk SDT group.

interstitial fibrosis. Similarly, both VEGF expression and microvessel density were decreased in diabetic mouse myocardia 5 wk after a single peritoneal injection of STZ (11). However, these reports did not address the cross-talk between cardiomyocytes and the coronary vasculature during cardiac growth. The reason for the discrepancy in the expression of VEGF in cardiac tissues of the STZ diabetic animals is unclear at present, but these reports and the present findings may suggest different mechanisms for the coronary capillary loss observed in diabetic hearts.